AD-A281 790

UMENTATION PAGE

Form Approved
OMB No 0704-0188

2. REPORT DATE	3. REPORT TYPE AND DATES COVERED
	THESIS/~~DISSERTATION~~

4. TITLE AND SUBTITLE
An Air Mass Transformation Model for Coastal Environments

5. FUNDING NUMBERS

6. AUTHOR(S)
Craig T. Sloan

7. PERFORMING ORGANIZATION NAME(S) AND ADDRESS(ES)
AFIT Student Attending:
Flordia State Univ.

8. PERFORMING ORGANIZATION REPORT NUMBER
AFIT/CI/CIA-
94-028

9. SPONSORING/MONITORING AGENCY NAME(S) AND ADDRESS(ES)
DEPARTMENT OF THE AIR FORCE
AFIT/CI
2950 P STREET
WRIGHT-PATTERSON AFB OH 45433-7765

10. SPONSORING/MONITORING AGENCY REPORT NUMBER

11. SUPPLEMENTARY NOTES

12a. DISTRIBUTION/AVAILABILITY STATEMENT
Approved for Public Release IAW 190-1
Distribution Unlimited
MICHAEL M. BRICKER, SMSgt, USAF
Chief Administration

12b. DISTRIBUTION CODE

13. ABSTRACT (Maximum 200 words)

94-22694

14. SUBJECT TERMS	15. NUMBER OF PAGES 93
	16. PRICE CODE

17. SECURITY CLASSIFICATION OF REPORT	18. SECURITY CLASSIFICATION OF THIS PAGE	19. SECURITY CLASSIFICATION OF ABSTRACT	20. LIMITATION OF ABSTRACT

94-028

THE FLORIDA STATE UNIVERSITY

COLLEGE OF ARTS AND SCIENCES

AN AIR MASS TRANSFORMATION MODEL FOR COASTAL ENVIRONMENTS

By

CRAIG T. SLOAN

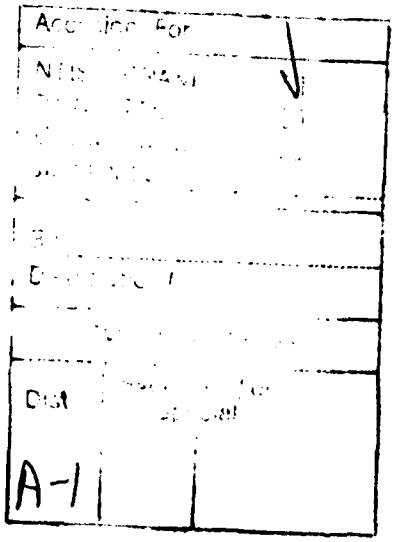

A Thesis submitted to the
Department of Meteorology
in partial fulfillment of the
requirements for the degree of
Master of Science

Degree Awarded:

Summer Semester, 1994

The members of the Committee approve the thesis of Craig T. Sloan defended on 26 April 1994.

Paul Ruscher
Professor Directing Thesis

Kevin Kloesel
Committee Member

T. N. Krishnamurti
Committee Member

This work is dedicated to my parents, Richard and Margaret, who always encouraged and fostered my love of science, and to my wife, Emmy; without whose patience and support, this work would not have been possible. I love you all very much.

Acknowledgments

I would like to thank my major professor, Dr. Paul Ruscher, for his guidance, support and patience during my stay at Florida State University. I also would like to thank the other members of my committee, Drs. Kevin Kloesel and T.N. Krishnamurti. They have both been a tremendous source of knowledge, both in the classroom and also on a more personal level.

A special thanks goes to fellow graduate students, Christopher Herbster, who has helped me out with many computer and science-related problems these past two years, and Gary Hodges for his help with programming and plotting figures. Jeff Ward and Jimmy Hudson must also be acknowledged for their help in solving many computer-related issues.

Finally, I would like to thank the United States Air Force for providing me with the opportunity to attend graduate school at Florida State University. I sincerely hope that the knowledge I have attained here will be helpful to the Air Force in future endeavors.

TABLE OF CONTENTS

LIST OF TABLES

LIST OF FIGURES

ABSTRACT

Frequently during winter, cold fronts move through the Gulf of Mexico region. Several days after the passage of the cold front, return flow develops along the Gulf Coast advecting modified continental polar air over the Gulf Coast states. An operational air mass transformation (AMT) model has been developed to forecast the thermodynamic structure of the planetary boundary layer (PBL) at coastal locations during these return flow events.

In order to test a new diagnosed 2 m temperature formulation, sixteen cases from 1993, where conditions at Tallahassee, FL, (TLH) were conducive for good radiational cooling were studied using a 1-d PBL model with a simple radiative parametrization and a surface energy balance. The forecasted minimum temperatures from the PBL model were compared to the forecasts from various large scale models and the actual minimum temperatures. The results were encouraging, as the PBL model was as highly correlated as the large scale models and contained a smaller bias with regard to forecasting the minimum temperature.

The same 1-d PBL model was adapted as an AMT model. Portions of two return flow events from January and February 1994, were modeled and several forecast parameters were compared to the observed parameters. The forecast parameters are well correlated with the observed parameters, especially for cases early in the return flow event. Several hypotheses are tested to explain

why the model performed better early in the return flow event. Three case studies are presented in more detail to further evaluate the model's performance.

CHAPTER 1. INTRODUCTION

A. Background

1. Return Flow Description

During the winter, cold, dry air masses frequently move south across the United States and plunge deep into the Gulf of Mexico. The coldest nights of the year in Tallahassee, FL, frequently occur 1-2 days after frontal passage as the ensuing anticyclone is usually situated nearby. This close proximity leads to a lessening of the pressure gradient and subsequent slackening of winds. This slackening of winds in conjunction with the clear, dry air of the modified polar airmass leads to strong radiational cooling at night and the associated cold temperatures. As the airmass moves over the Gulf, significant airmass modification occurs (Henry and Thompson 1976), with a substantial flux of heat and moisture being transferred from the Gulf to the atmosphere.

Over time, the high pressure system tracks eastward and a subsequent southerly flow develops along the Gulf Coast. Some of the air associated with this flow is air that originated in the cold, dry airmass and has undergone modification before "returning" to land as a result of the synoptic circulation. This process is commonly referred to as "return flow" (Crisp and Lewis 1992), and the whole process of cold air outbreaks followed by return flow has been referred to by Crisp and Lewis (1992) as the return-flow cycle.

This northward transport of moisture can cause major problems for operational forecasters along the Gulf Coast in the form of low ceilings and visibility associated with fog, as well as severe weather (Crisp and Lewis 1992). With forecasting problems like these, it is no wonder that operational forecasters pay particular importance to the onset of return flow events, as evidenced by the numerous references to this phenomenon in forecast discussions issued by National Weather Service Offices in the Gulf Coast states.

2. Numerical Model Performance During Return Flow

a) Nested Grid Model

Thus, it is important to accurately predict the thermodynamic characteristics of the airmass associated with the return flow. Unfortunately, as shown by Janish and Lyons (1992) the National Meteorological Center's (NMC) NGM does not predict the moisture structure of the return flow airmass well at all (Fig. 1), nor does it accurately predict the temperature inversion, either over the Gulf or over land (Fig. 2). This is a serious problem as it leads to a poor forecast of the vertical moisture profile and an inaccurate forecast of the depth of inland penetration of moisture during the return flow (Janish and Lyons 1992). Overall, their study showed, using data from the 1988 Gulf of Mexico Experiment (GUFMEX) and NGM forecasts from that time, that NGM moisture forecasts during return flow cycles are dominated by advective processes rather than air mass modification processes.

Janish and Lyons accomplished this in the following manner. They

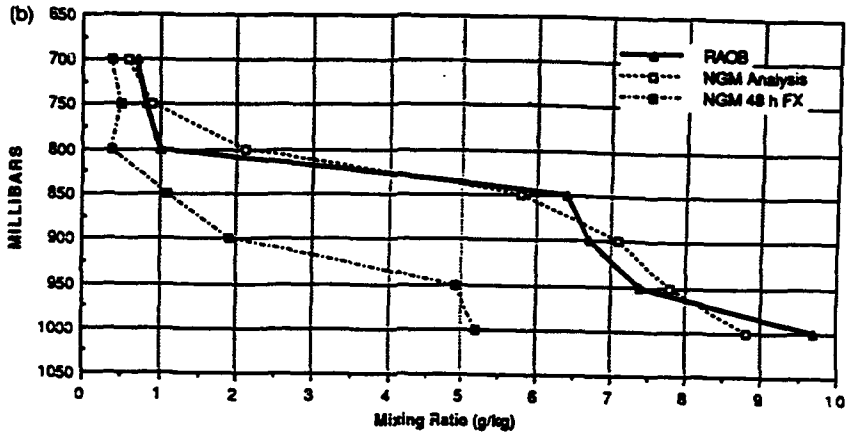

Fig. 1. Vertical profile of mixing ratio obtained from RAOB (Lake Charles, LA), NGM 48-hour forecast, and NGM analysis for a return flow event. (From Janish and Lyons 1992)

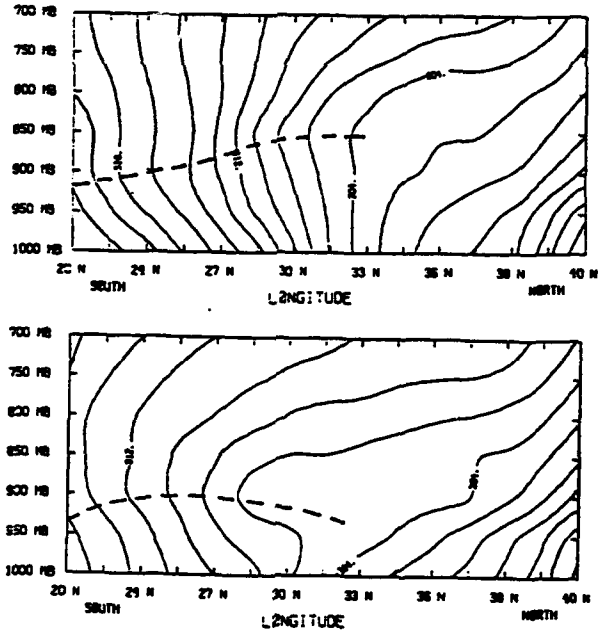

Fig. 2. South-north cross sections (along 94 °W) showing NGM analysis (top) and NGM forecast (bottom) for θ_e (K) at the same time during an average return flow event. Dashed line indicates top of boundary layer. Latitude is incorrectly marked as longitude. (From Janish and Lyons 1992)

constructed a composite return flow event, by averaging 7 return flow events from the winter of 1988. They then compared the NGM analysis with the NGM 48-hour forecast, for this composite return flow event, at the time of the maximum dry, cold advection into the Gulf. They then advected the 4 g kg^{-1} isohume along each grid point via a trajectory until the beginning of the return flow phase and determined its position (Fig. 3). The NGM forecast of the 4 g kg^{-1} is very close to what would be expected due to pure advection, whereas the NGM analysis for the same time shows a much different position for the same isohume.

Janish and Lyons determined that, in actuality, approximately 60-70% of the total moisture change in an airmass during an average return flow event is due to air mass modification. Whereas, only 20-30% of the total moisture change is due to modification in the NGM 48-hour forecasts, with advection being the dominant process. According to Janish and Lyons, this problem in the NGM, with advection dominating modification, results in the moisture gradient associated with the cold front being advected past the domain of the NGM grid. As a result, once the return flow begins, the air being advected northward is much too dry (Fig. 3). However, their study was performed before the recent changes to the NGM which included a southward extension of the grid to Panama and the addition of stability-dependent fluxes over water (Janish and Lyons 1992). No study has been performed to determine the effect of these changes on the ability of the NGM to forecast return flow events.

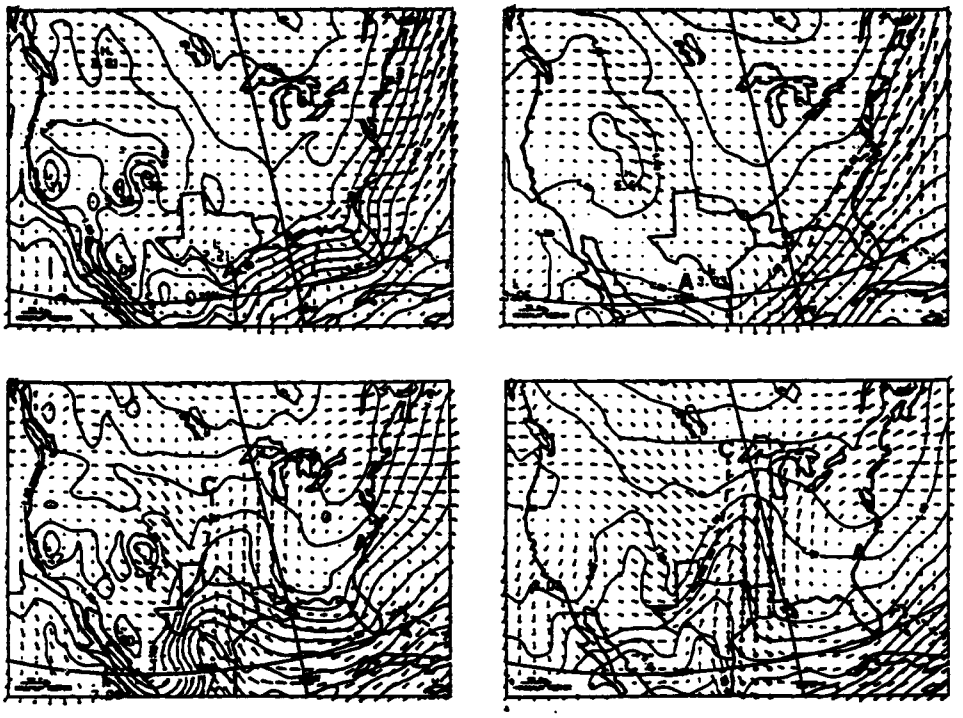

Fig. 3. Mixing ratio and wind at 950 hPa for NGM analyses (left) and NGM forecasts (right) at the start of an average return flow event (top) and at the time of maximum return flow (bottom). The dashed line in the top panels indicates the position one would expect the 4 g kg^{-1} to be based purely on advection. (From Janish and Lyons 1992)

b) MESOSCALE MODELS

There have been several attempts recently to more accurately forecast the airmass modification that occurs during a return flow cycle (Mailhot 1992; Burk and Thompson 1992; Thompson and Burk 1993). Mailhot (1992) used a mesoscale version of the Canadian regional finite-element model to simulate a return-flow event that occurred during GUFMEX. A complete description of

the model is given in her paper. Mailhot also asserts that the dominant process in the boundary layer is not advection, but rather it is the surface fluxes of heat and moisture, as well as the subsequent distribution of the fluxes via turbulent mixing, which dominates the moistening of the planetary boundary layer (PBL). In order to show this, Mailhot ran her model twice - once with surface fluxes included, and once with no surface fluxes included. The effect of neglecting surface fluxes is clear. Figure 4 shows 36-hour forecasts of potential temperature and mixing ratio for both model runs. This is approximately the start of the return flow phase. The run without fluxes maintains sharp gradients of moisture and temperature, while the run with surface fluxes relaxes these gradients as the air mass modifies. Also note the warming and moistening that takes place in the model run with surface fluxes. This is consistent with what Janish and Lyons (1992) showed - without an accurate description of the surface energy fluxes, the temperature and moisture gradient associated with the cold front is not allowed to relax due to the modification of the airmass by the warm waters of the Gulf.

c) AIRMASS TRANSFORMATION MODEL

1) Description

Burk and Thompson (1992) as well as Thompson and Burk (1993) have used what is known as an air mass transformation (AMT) model to try and forecast the initial modification of continental, polar (cP) air as it moves over the Gulf of Mexico, as well as the subsequent return flow of the modified air. A

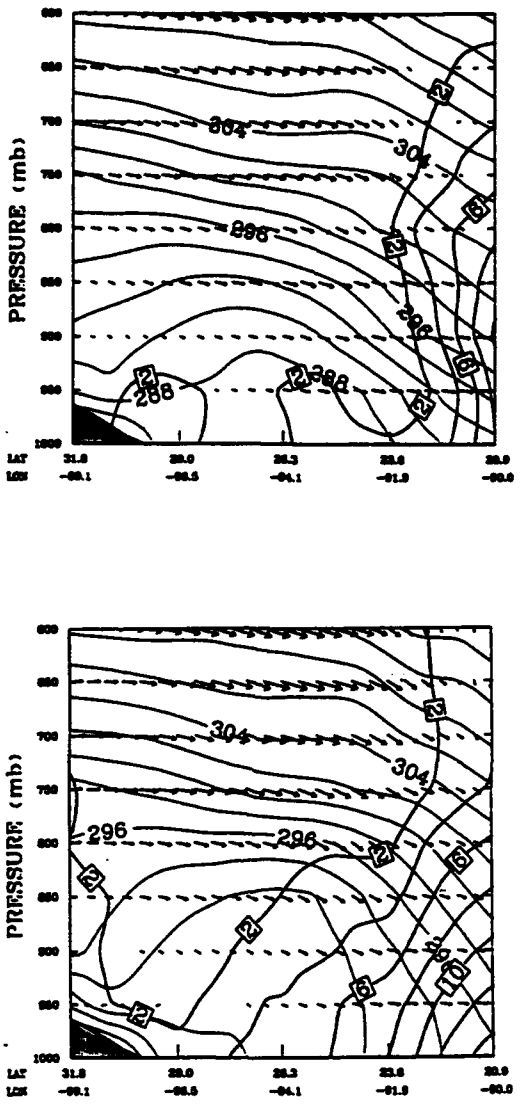

Fig. 4. Forecasts of θ (K) and q (g kg^{-1}) for model run without surface fluxes (top) and with surface fluxes included (bottom). Values of isohumes are denoted in boxes. (From Mailhot 1992)

description of their AMT model will be followed by a summary of their results.

Burk and Thompson's AMT model is a high resolution, one-dimensional column model with 40 grid points from the surface to 4500 m. The model is designed to move along a low-level trajectory in a Lagrangian manner. The model is initialized from a sounding derived from a mesoscale model at the source point of the low-level trajectory, or with a nearby radiosonde. Back trajectories are calculated using a mesoscale model at 6 different levels between the surface and 500 hPa. This means that all the trajectories arrive at the forecast point at the same time. Often in return flow events, air at upper levels originates in different areas than does air near the surface. A favorite source region for upper level air that arrives in Brownsville, TX, during return flow events is the Mexican Plateau. Obviously, initializing the model at 700 hPa over the Gulf of Mexico would lead to incorrect results. Burk and Thompson account for differential advection at upper levels by including a forcing term which is added to the prognostic equations for potential temperature and moisture. In the absence of diabatic effects, the parcel of air arriving at the termination point of the trajectory will have the same conservative properties as it did upstream, taking into account adiabatic warming and cooling associated with subsidence and ascent.

The horizontal wind components are also initialized from the mesoscale model and are "nudged" towards the values forecasted from the mesoscale model during the AMT model run. Burk and Thompson allow the winds to depart from the mesoscale forecast in the boundary layer to take into account turbulent fluxes, but above the boundary layer, where turbulent fluxes are negligible, they

do not.

To summarize, after initializing the model using either an actual, nearby radiosonde sounding, or a mesoscale model derived sounding, the AMT model is advected along the lowest trajectory. If, while being advected, it is over water, the surface temperature is prescribed as the sea surface temperature. Physics that occur at every time step include equations for mean wind, potential temperature and moisture. Also, liquid water content and stable precipitation rates are diagnosed.

2) Results of Immediate Post-frontal Modification

Burk and Thompson (1992) looked at the modification of the cP air mass as it initially was advected over the Gulf of Mexico. They calculate 12-hour back trajectories that arrive at a point in the Gulf of Mexico at 0000 UTC, 22 February 1988 (Fig. 5). The AMT model was initialized using the 1200 UTC, 21 February sounding from Boothville, LA (BVE). As would be expected, the planetary boundary layer (PBL) warms and moistens with time as the model moves out into the Gulf of Mexico (Fig. 6). Also, the boundary layer height increases during the 12 hour forecast. Burk and Thompson (1992) attribute these changes to the strong surface fluxes which would result from cold, dry air moving over warm water.

Burk and Thompson (1992) also compare vertical profiles of potential temperature and specific humidity at the termination point of the trajectories (Fig. 7). The profiles are from a dropsonde that occurred at that point, as well as from

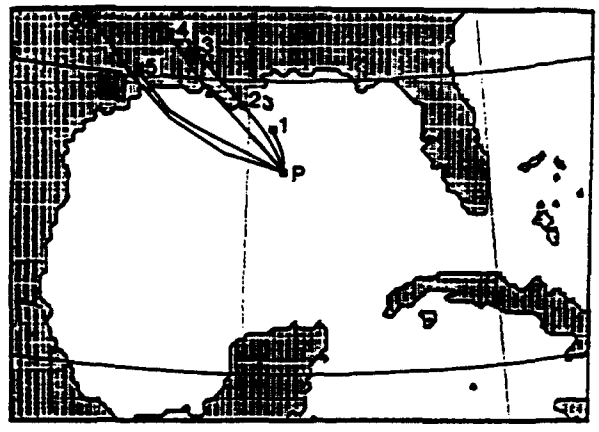

Fig. 5. Twelve-hour trajectories arriving at point P at 00 UTC, 22 February 1988. Trajectory levels range from surface (1) to 500 hPa (6) when they arrive at point P. (From Burk and Thompson 1992)

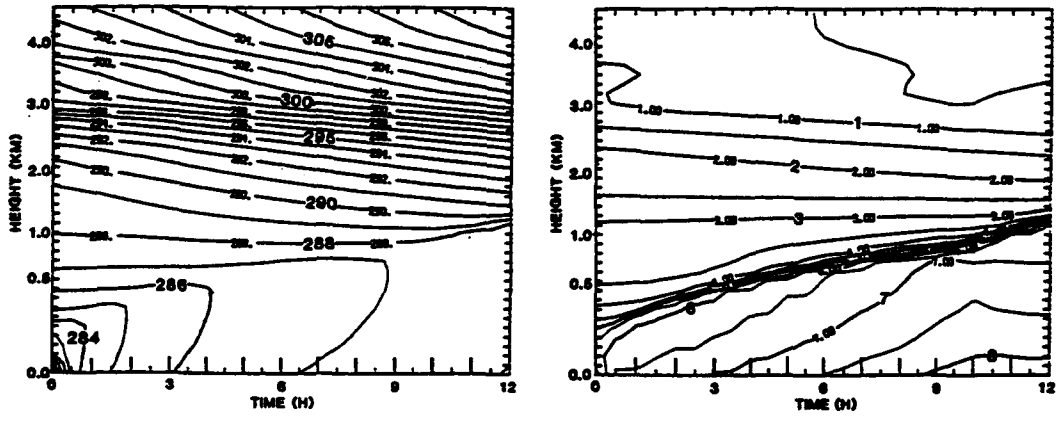

Fig. 6. Time sections of potential temperature (K) (left) and specific humidity (g kg^{-1}) along trajectory 1. (From Burk and Thompson 1992)

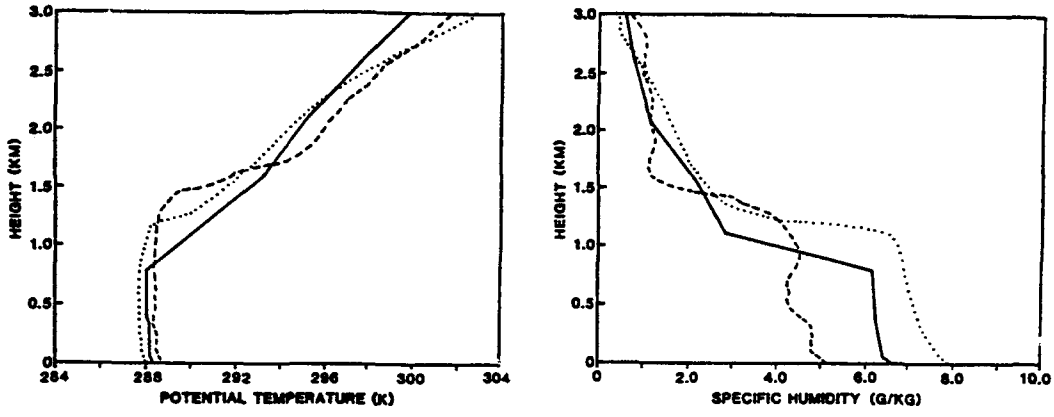

Fig. 7 Potential temperature (K) (left) and specific humidity (g kg^{-1}) (right) profiles for point P valid 00 UTC, 22 February from AMT model (dotted), from a dropsonde at 1900 UTC, 21 February (dashed), and a mesoscale model valid at 1900 UTC, 21 February (solid). (From Burk and Thompson 1992)

forecasts from the AMT model and a mesoscale model. Although the height of the boundary layer forecasted by the AMT model is about 300 m less than the observed boundary layer, the AMT model provides a much better forecast than does the mesoscale model. Also, the AMT model is much too moist when compared to the profile obtained from the dropsonde. However, Burk and Thompson feel that since the dropsonde moisture profile is similar to the initial BVE profile, and did not show any signs of moistening, it is not realistic, and disregard it.

3) Return Flow Forecasts

Thompson and Burk (1993) use the same AMT model to try and forecast

return flow during the same time period as their previous study. For this study, they calculate back trajectories for 60 hours, which encompasses the entire cycle of initial flow of air out over the Gulf to the return flow (Fig. 8). Note that the 1000 hPa trajectory starts at Brownsville, TX, (BRO) and arrived just offshore of BRO. The model was initialized using the Brownsville sounding from 0000 UTC, 21 February 1988.

As the model moves from land to warmer water, the boundary layer warms and grows in the first 12 hours (Fig. 9). The boundary layer continues to grow, but does not warm in the next 12 hours. Burk and Thompson attribute this to cloud-top radiative cooling offsetting the warming from the surface heat flux and entrainment of high potential temperature air above the boundary layer.

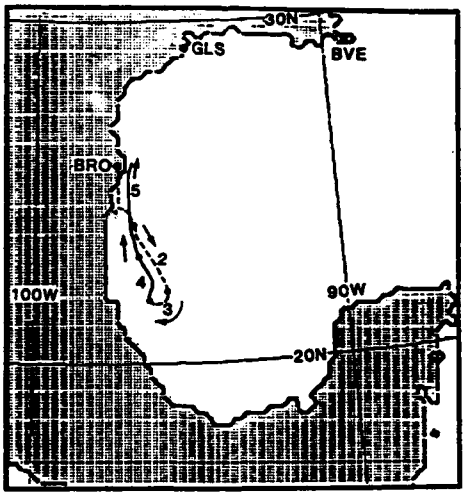

Fig. 8. Sixty hour 1000 hPa trajectory starting at Brownsville, TX, at 00 UTC, 21 February 1988. Numbers indicate each 12 hour position of the trajectory. (From Thompson and Burk 1993)

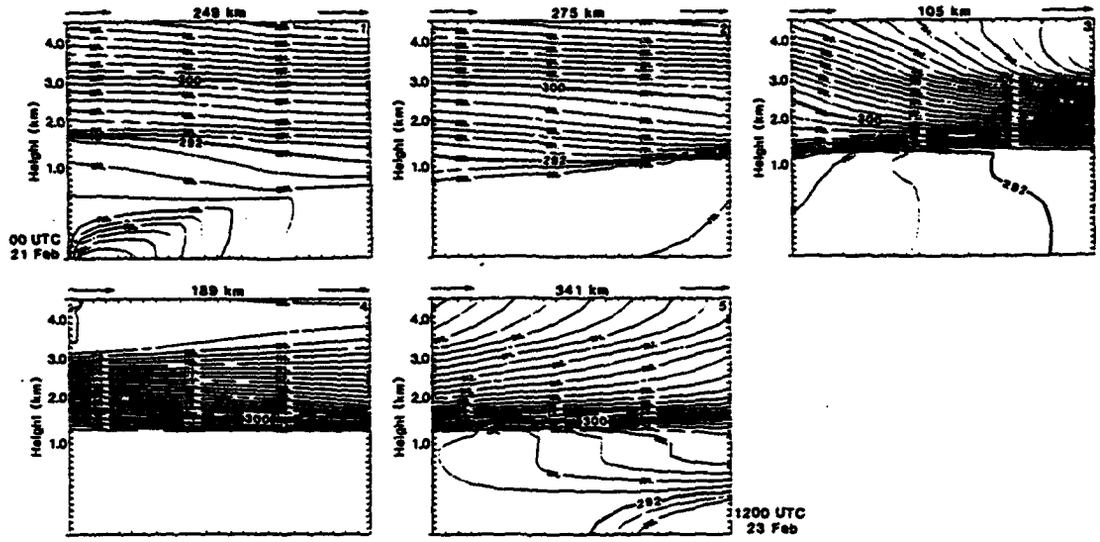

Fig. 9. Twelve-hour time sections of potential temperature (K) for the 5 segments shown in Fig. 8. The first section begins at 00 UTC, 21 February, and the last section ends at 1200 UTC, 23 February. (From Thompson and Burk 1993)

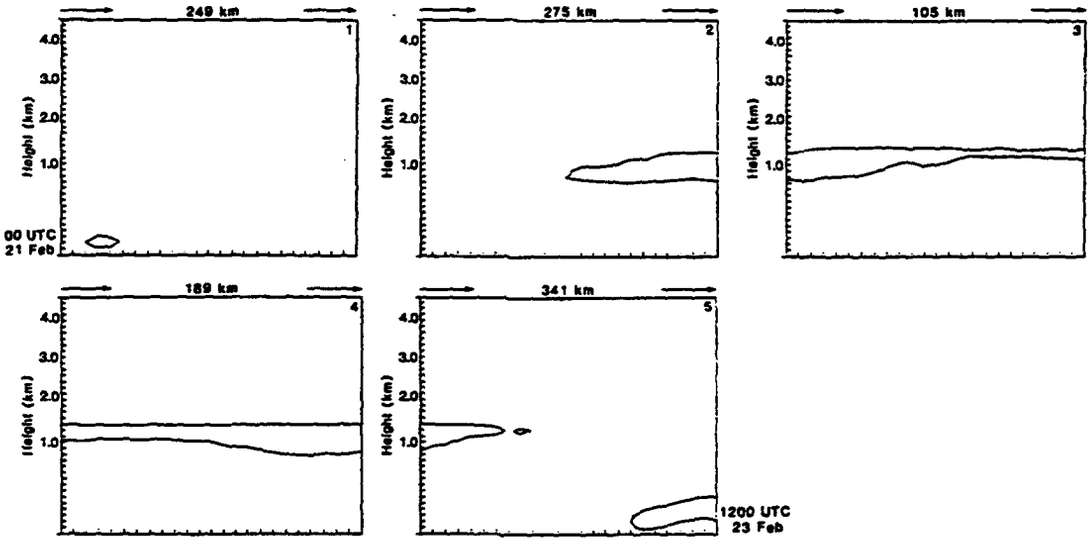

Fig. 10. As in Fig. 9, but for the nonzero isopleth of cloud liquid water. (From Thompson and Burk 1993)

Figure 10 shows the time section of cloud liquid water content. The region enclosed by the line indicates nonzero cloud liquid water content, indicative of cloudy regions. The third 12 hour period shows the height of the boundary layer leveling out and the temperature increasing. Burk and Thompson attribute this to more of the surface heat flux going into warming instead of deepening the boundary layer. The last period shows rapid cooling of the surface layer as the AMT model moves over colder waters. In fact, this surface layer decouples from an upper mixed layer which is warmed by subsidence which leads to the dissipation of the upper cloud layer.

Time-sections of specific humidity show similar results (Fig. 11). As the model moves southward over warmer waters, the specific humidity increases and only decreases in the last 6 hours of the model run as the boundary layer

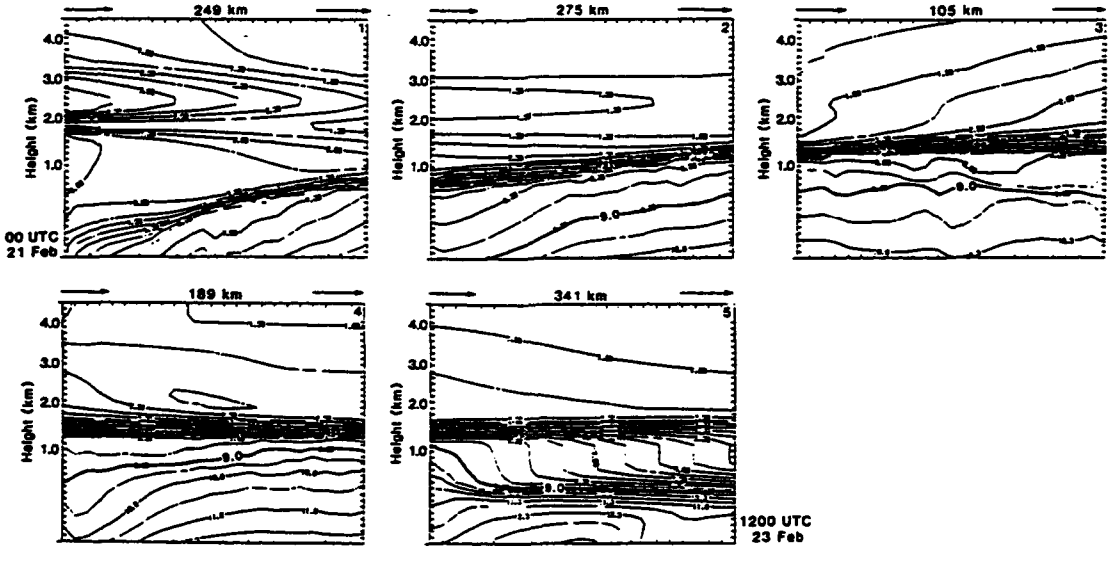

Fig. 11. As in Fig. 9, but for specific humidity (g kg^{-1}). (From Thompson and Burk 1993)

cools.

Thompson and Burk (1993) compare the vertical profiles of temperature and specific humidity for the initial sounding, the final model sounding (1200 UTC, 23 February 1988), and the sounding at Brownsville for 1200 UTC, 23 February 1988 (Fig. 12). One problem with this comparison is that the model profile occurs over water where the nocturnal radiative cooling that occurred over land can not be represented. This results in the failure to see a mixed layer in the Brownsville sounding which the model predicts. Also, above the mixed layer, the model predicts too deep of an inversion. These features can also be seen in the specific humidity profiles. Overall, the model does a respectable job of forecasting the changes in potential temperature and specific humidity.

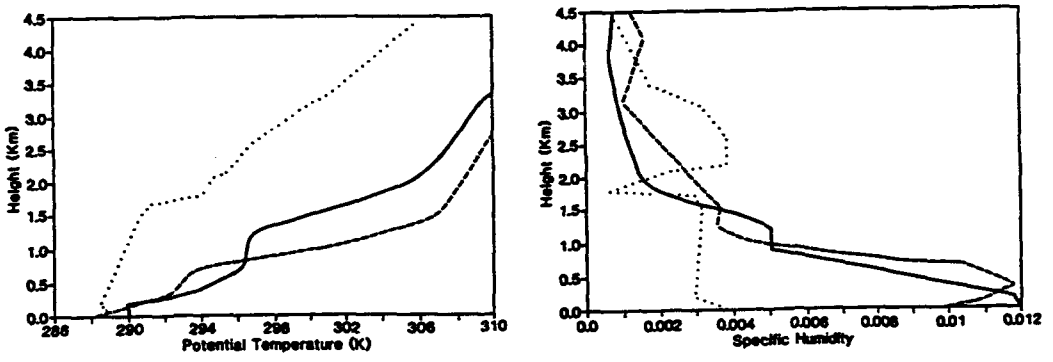

Fig. 12. Profiles of potential temperature (K) (left) and specific humidity (g kg^{-1}) (right). Shown are results from the AMT model (solid) and the Brownsville sounding (dashed), both valid at 1200 UTC, 23 February 1988. Also shown are the profiles used to initialize the model (dotted). (From Thompson and Burk 1993)

B. Goals of Present Study

The goals of the present study are two-fold. First, as discussed earlier, after cold frontal passage, a synoptically quiet period (temperature and moisture advection are minimal) occurs for a day or two. This period is perfectly suited for using the Oregon State University (OSU) one dimensional (1-d) PBL model to try and forecast minimum temperatures at a location such as the Tallahassee Regional Airport (TLH). With little advection occurring, the PBL model should perform well, as it contains a fairly sophisticated surface energy balance and formulation for the very stable PBL. This model will be discussed in the next chapter.

However, once the return flow begins, advection does become important making the PBL model less useful as a forecasting tool. Thus, the second goal is to develop the PBL model as an AMT model to try and forecast the thermodynamic structure of the boundary layer. In adapting the OSU model as an AMT model, the approach used by Holtslag *et al.* (1990) will be followed. Details of this adaptation will also be discussed in the next chapter. It is felt that the excellent boundary layer formulation in the OSU model will lead to a useful AMT model of somewhat different design than that of Burk and Thompson (1992).

CHAPTER 2. METHODOLOGY

A. INTRODUCTION

The models used in this study are a locally modified OSU 1-d PBL model, version 1.0.4 (Ek and Mahrt 1991), and the PBL model adapted as an AMT model. The changes to the OSU model included the method of determining the 2 m air temperature and the 10 m wind. These will be discussed in more detail later in this chapter. The OSU model will be discussed first along with the aforementioned changes to it. Then, a discussion of how the model was adapted for use as an AMT model will be presented.

B. PBL Model

The PBL model is a coupling of a planetary boundary layer model (Troen and Mahrt 1986) with a two-layer soil model (Mahrt and Pan 1984) and a simple plant canopy model (Pan and Mahrt 1987). One of the primary advantages of the model is that the equations used in the model are complex enough to closely approximate the important physical processes that occur in the development of the boundary layer, yet the equations are also simple enough that the model can be run in just a few minutes (Ek and Mahrt 1991) on a workstation or modern PC. One of the primary disadvantages of the model is

that since it is a one-dimensional model, horizontal advection and other large scale processes are not accounted for. Advection is obviously an important process during periods of large synoptic forcing. This is the motivation for adapting the PBL model as an AMT model. Then, a high-resolution boundary layer model which incorporates advection would be available that could be run on a PC or workstation in just a few minutes.

1. Two-layer Soil Model

a) SOIL HYDROLOGY

The soil model consists of two layers. The upper layer is 5 cm thick, while the lower layer is 95 cm thick. The upper layer responds more to diurnal forcing, while the lower layer is more responsive to seasonal changes, such as soil water storage (Pan and Mahrt 1987). There are 11 different types of soil that can be prescribed for use in the model; however, the same soil type must be used in both soil layers. The soils that were predominately used in this study were sandy clay loam, sandy clay, and clay. The choice of soil did not greatly affect the forecast structure of the PBL for a control case described in chapter 3 (Fig. 13).

For initialization, the model requires only the soil type, wilting point, and volumetric water content be input. Initially, the volumetric water content of both soil layers is set equal. Volumetric water content is the most important prognostic variable in the soil model, as it is an important factor in determining evaporation of soil moisture, which in turn is an important factor in determining

the structure of the PBL (Fig. 14). The prognostic equation for volumetric water content (Θ) is as follows:

$$\frac{\partial \Theta}{\partial t} = \frac{\partial}{\partial z}\left(D(\Theta)\frac{\partial \Theta}{\partial z}\right) + \frac{\partial K(\Theta)}{\partial z} \qquad (1)$$

where the coefficients of diffusivity (D, units of $m^2\ s^{-1}$) and hydraulic conductivity (K, $m\ s^{-1}$) are functions of the volumetric water content (Mahrt and Pan 1984). These two coefficients can not be treated as constants because they can vary by several orders of magnitude depending on whether the soil is extremely dry or moist.

Evaporation at the surface of the soil is referred to as direct evaporation. It is a function of diffusivity, hydraulic conductivity and the vertical moisture

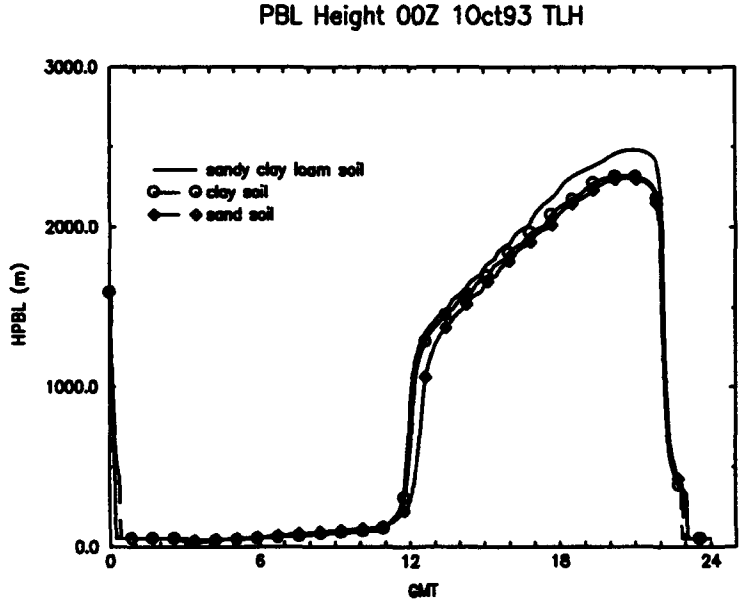

Fig. 13. Dependence of PBL height on input soil. Input soils used were sand, clay, and a sandy clay loam.

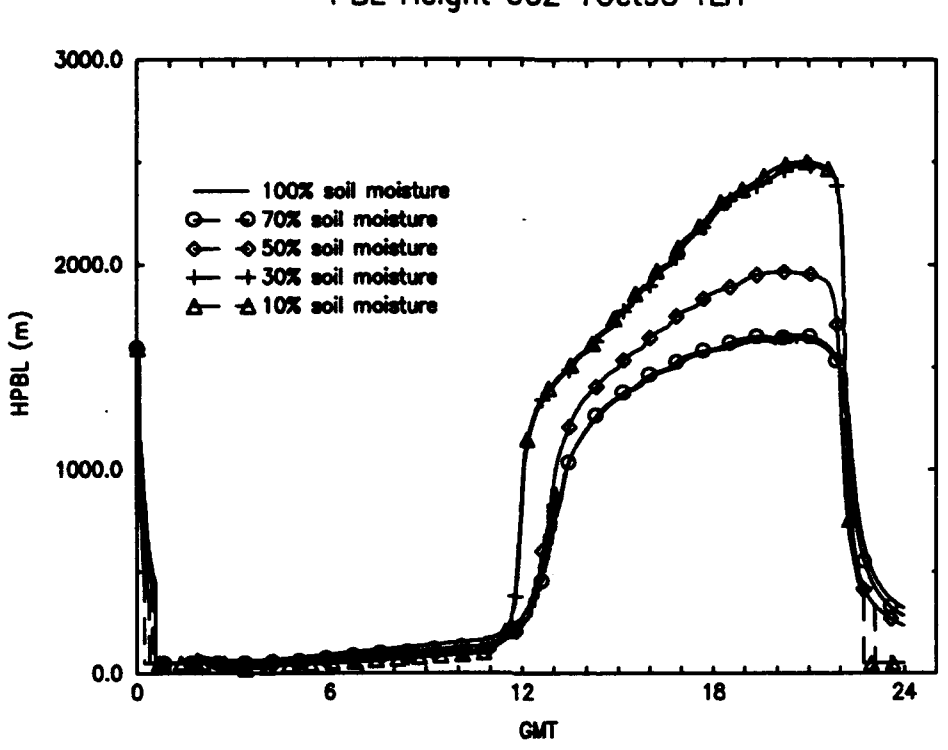

Fig. 14. Dependence of PBL height on input soil moisture. Input soil moisture values range from 100% to 10% of saturation.

gradient. The equation for direct soil evaporation at the surface is given by (Ek and Mahrt 1991)

$$E_{soil} = \left[-D(\Theta)\left(\frac{\partial \Theta}{\partial z}\right)_0 - K(\Theta)_0 \right] \qquad (2)$$

where the subscript zero refers to the value at the air-soil interface.

b) SOIL THERMODYNAMICS

Soil thermodynamics are governed by the following prognostic equation

for soil temperature (T) (Ek and Mahrt 1991):

$$C(\Theta)\frac{\partial T}{\partial t} = \frac{\partial}{\partial z}K_T(\Theta)\frac{\partial T}{\partial z} \tag{3}$$

where C is the volumetric heat capacity and K_T is the thermal conductivity of the soil, and both are functions of the volumetric soil water content. The heat capacity is a linear function of Θ while the thermal conductivity is similar to the diffusivity and hydraulic conductivity in that it is highly nonlinear and varies by several orders of magnitude between dry and wet soil conditions (Ek and Mahrt 1991).

The soil heat flux, G, is the upper boundary condition for the soil thermodynamic model, and it is also plays an important role in the surface energy budget. It is determined by (Ek and Mahrt 1991):

$$G = K_T(\Theta)\left(\frac{\partial T}{\partial z}\right)_{z=0} \tag{4}$$

The role of vegetation, and how it interacts with the soil model is discussed in the next section.

2. Plant-Canopy Model

Transpiration from plants represents an important part of the moisture budget in the boundary layer which underscores the need to accurately represent the process in boundary layer modeling. Another important effect

plants have on boundary layer development is the evaporation of free water by the plant canopy. The relationship of these effects in the overall evaporation budget is

$$E = E_{dir} + E_T + E_c \tag{5}$$

where E_{dir} is the direct evaporation of moisture from the soil; E_T is transpiration, and E_c is the evaporation of free water by the plant canopy (Pan and Mahrt 1987)

Plants are also important because they reduce direct evaporation from the soil by shading and also by reducing wind speed near the ground. These effects are included together (for simplicity) in a shading factor σ_f where

$$E_{dir} = E_{soil}\,(1-\sigma_f) \tag{6}$$

and E_{soil} is obtained from (2) (Pan and Mahrt 1987).

Transpiration is a function of plant density and soil moisture. In the OSU model, transpiration is included via the following formulation from Pan and Mahrt (1987):

$$E_T = E_p k_v \sigma_f \left[\frac{z_1}{z_2} g(\Theta_1) + \frac{z_2 - z_1}{z_2} g(\Theta_2)\right] \left| 1 - \left(\frac{c^*}{s}\right)^n \right| \tag{7}$$

where z_1 is the depth of the first soil layer (5 cm) and z_2 is the depth of the entire

soil layer (1 m). E_p is the potential evaporation which is calculated by (Ek and Mahrt 1987):

$$E_p = \rho_0 C_h \left(q_s^* \left(\theta_s' \right) - q_2 \right) \tag{8}$$

where C_h is the exchange coefficient for heat and q_2 is the specific humidity at the second model level. The variable $q_s^*(\theta_s')$ is the saturation specific humidity that would occur for a surface temperature of a saturated surface.

The parameter k_v is a scaling factor known as the plant resistance factor. It can very between 0 and 1, and is set to 0.4 in the model. This constant is an attempt to take into account the reduction in transpiration due to internal plant physiology (Ek and Mahrt 1991).

The transpiration rate function, g(Θ) also varies between 0 and 1. It is zero if the actual water content is below the wilting point (Θ_{wilt}) which is defined as the Θ value where transpiration stops (Mahrt and Pan 1984). It is 1 if the actual value of Θ is greater than the Θ value where transpiration begins to decrease due to soil drying (Θ_{ref}). If the actual value of Θ lies between Θ_{ref} and Θ_{wilt}, g(Θ) is defined as

$$g(\Theta) = \frac{\Theta - \Theta_{wilt}}{\Theta_{ref} - \Theta_{wilt}}. \tag{9}$$

C^* is the canopy water content, and S is the canopy water capacity (2 mm in the model). These are included to take into account the reduction of transpiration from surfaces covered with a water film (Pan and Mahrt 1987). The

power n is set to 0.5 based on work by Leyton *et al.* (1967).

The evaporation of free water by the canopy, E_c, is defined as (Pan and Mahrt 1987)

$$E_c = \sigma_f \left(\frac{C^*}{S} \right)^n E_p . \tag{10}$$

Combined with the previously described soil model, this plant-canopy model provides a realistic representation of the surface processes that affect development of the PBL.

3. Boundary Layer Model

The boundary layer portion of the model was first developed by Troen and Mahrt (1986), and is extensively discussed in Ek and Mahrt (1991). The model consists of a high-resolution vertical grid: specifically, there are up to 70 levels from the surface to 10,000 m with a grid spacing of 20 m in the lowest 400 m, 50 m from 400 m - 1400 m, 100 m from 1400 m - 2000 m, 200 m from 2000 m - 4000 m, 300 m from 4000 m - 4600 m, 400 m from 4600 m - 5000 m, and 500 m from 5000 m - 10,000 m. The time step used was 3 minutes.

a) PROGNOSTIC EQUATIONS

The model forecasts the tendencies due to turbulent mixing of specific humidity (q), potential temperature (θ), and the horizontal component of wind

($\vec{V_h}$). The equations used in the model are

$$\frac{\partial \vec{V_h}}{\partial t} = 2\Omega \times \vec{V_h} + \left(\frac{\partial}{\partial z} K_m \frac{\partial \vec{V_h}}{\partial z} \right) - w \frac{\partial \vec{V_h}}{\partial z} \tag{11a}$$

$$\frac{\partial \theta}{\partial t} = \frac{\partial}{\partial z} \left[K_h \left(\frac{\partial \theta}{\partial z} - \gamma_\theta \right) \right] - w \left(\frac{\partial \theta}{\partial z} \right) \tag{11b}$$

$$\frac{\partial q}{\partial t} = \frac{\partial}{\partial z} \left(K_h \frac{\partial q}{\partial z} \right) - w \left(\frac{\partial q}{\partial z} \right). \tag{11c}$$

Thus the only terms included in the prognostic equations for θ and q are vertical advection and vertical diffusion due to turbulent mixing. The Coriolis parameter is included in the prognostic equation for $\vec{V_h}$. The variables K_m and K_h are coefficients of diffusivity for momentum and heat, respectively. The term, γ_θ, is the counter-gradient correction for potential temperature (Deardorff 1966). It is zero if the boundary layer is stable, and its unstable parametrization is given by

$$\gamma_\theta = C \frac{(\overline{w'\theta'})_s}{w_s h} \tag{12}$$

where h is the boundary layer height, C is a constant set to 8.5 (Holtslag 1987), and w_s is a vertical velocity scale of the boundary layer. The term $(w'\theta')_s$ is the vertical eddy heat flux at the surface and is parameterized in the model using a nondimensional profile function for heat. This term is necessary due to the fact that in a convective boundary layer, large eddies exist which transport heat from

hot to cold regions, regardless of what the background gradient of temperature is (Stull 1988).

b) SURFACE LAYER

Surface fluxes of heat, momentum and moisture are related to T, $\vec{V}_h$ and q at the lowest model level by parametrization schemes developed by Mahrt (1987) for the stable case and by Louis *et al.* (1982) for the unstable case. The surface fluxes are given by

$$u_*^2 = C_m \left| \vec{V}_2 \right| \tag{13a}$$

$$(\overline{w'\theta'})_s = C_h(\theta_s - \theta_2) \tag{13b}$$

$$(\overline{w'q'})_s = C_h(q_s - q_2). \tag{13c}$$

The variables C_m and C_h are the surface exchange coefficients for heat and momentum, respectively, and are stability dependent. They are functions of $|V_2|$, the height of the first model level, the roughness length and the bulk Richardson number which will be described in the next section. The subscript 2 denotes the value at the second model level (first above the surface), and the subscript s denotes values at the surface.

c) BOUNDARY LAYER HEIGHT

The height of the boundary layer is determined by specifying a critical bulk Richardson number, Ri=1.0, such that

$$h = Ri\frac{\theta_{v2}\left|\vec{V}(h)\right|^2}{g(\theta_v(h)-\theta^*_{v2})} \tag{14}$$

where h denotes the variable is to be evaluated at height, h. The term θ_{v0}^* is used to represent a low-level potential temperature and is defined as θ_{v0} if the boundary layer is stable, and as

$$\theta^*_{v0} = \theta_{v0} + C\frac{(\overline{w'\theta'_v})_s}{w_s} \tag{15}$$

under unstable conditions. The variable w_s was defined in conjunction with (12). This term is added to take into account that the virtual potential temperature at the top of the surface layer is enhanced by thermal effects in an amount proportional to the surface sensible heat flux ($\overline{w'\theta'_v}$) when the boundary layer is unstable (Ek and Mahrt 1991).

During each time step, the value of h is increased until the relationship in (14) is met. During the day, this will occur just above the well-mixed region (Troen and Mahrt 1986).

4. Data for PBL Model

A majority of the data required to run the model are available via the GEneral Meteorological PAcKage (GEMPAK) which is a graphical interface allowing access to meteorological data. The model requires an initialization sounding containing T, q, u, v, w and z as well as the surface pressure be inputted. The variables T, q, u and v are easily retrieved from nearby radiosonde data. The vertical velocity must be calculated, however. GEMPAK does provide a method for calculating the vertical velocity using the O'Brien method (O'Brien 1970). All five variables are then interpolated from their actual vertical levels to the grid levels defined earlier using a least-squares method. It should be noted that the maximum value of w is capped at 1 cm/s in the model. This is so that the vertical advection terms in (11) do not become the dominant terms within the boundary layer. This restriction is justified, as 1 cm/s is the a good synoptic scale value for the vertical component of the wind.

It should also be noted that the start time of the model is one hour earlier than the official sounding time. This is done to take into account that all radiosondes are launched approximately an hour before the official time of the sounding. Thus for the purposes of the PBL, a 00 UTC sounding is really a 2300 UTC sounding.

As stated earlier, soil moisture must be input into the model. Unfortunately, there are no real-time reported soil moisture values available. This is a potential problem as the model is sensitive to the value of the input soil moisture (Fig. 14). What has been done here is to make an educated guess

about the soil moisture. The soils in the areas of the study have a high infiltration rate. Since the model is only being used during periods of synoptically quiet activity, 1-3 days of drying have usually taken place before the model is run. Also, experience with adjusting soil moisture values, and examining the resultant effect on the forecasted boundary layer structure has led to a value of 30% of saturation being used in almost all studies. If an extremely wet period did occur prior to the days used in the study, then the soil moisture was adjusted upwards. The converse is true for long dry periods that may have occurred. The soil type must also be input, but as was seen earlier, the model is not as sensitive to changes in soil type as it is to soil moisture (Fig. 13).

Additional parameters that can be adjusted include roughness lengths for heat and momentum (0.01 and 0.1 for these studies), albedo (0.23 for land, 0.1 for water) as well as the various vegetation variables discussed earlier.

C. CHANGES TO OSU PBL MODEL

During the course of this study, several parametrizations in the model were discovered to be unreliable under certain meteorological conditions. The next section describes what changes were made to the 1-d model.

1. Calculation Of 2 m Temperature And 10 m Wind Speed

One of the problems with the OSU model that was discovered during the minimum temperature study was that during times of transition from unstable to

stable conditions, when the wind speed dropped to almost zero, the *diagnosed* 2 m air temperature would become unrealistic (Fig. 15). In fact, diagnosed air temperatures of -600 C were not uncommon in these cases. The reason for this can be seen in the original OSU formulation for the calculation of the 2 m temperature (Holtslag 1987)

$$T_{air} = f(T_2, -1/L, T_{sfc}, z(T_2)) \tag{16}$$

where L, the Monin-Obukhov length is determined by:

$$L = \frac{\theta u_*^3}{\overline{\theta' w'} gk} \tag{17}$$

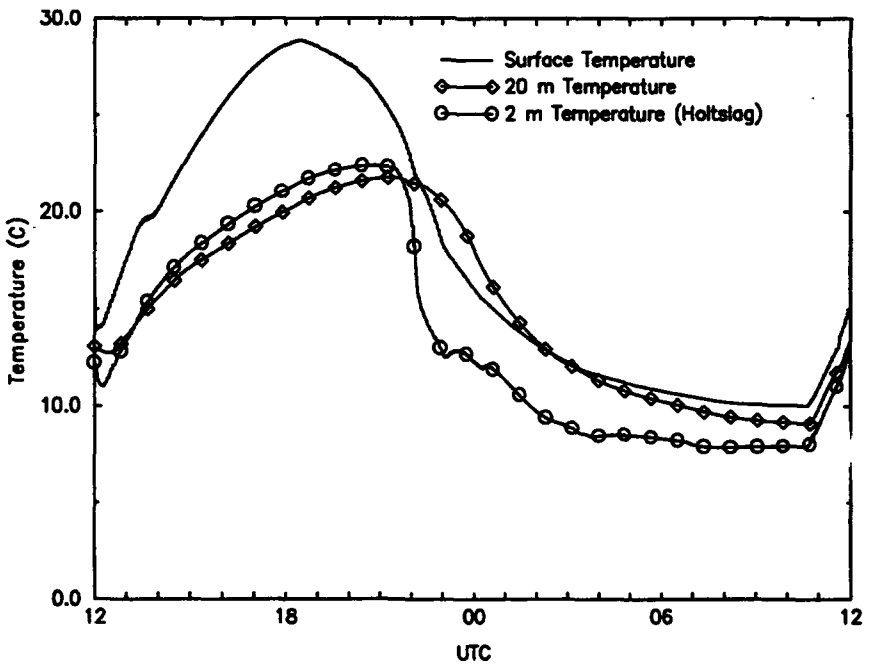

Fig. 15. Surface, 20 m, and 2 m temperatures for a composite 24 hour model run. Composite consists of 5 cases from TLH and Corpus Christi, TX (CRP) from various times of year.

and the friction velocity is defined as:

$$u_*^2 = \sqrt{(\tau_x^2 + \tau_y^2)} \tag{18}$$

where the wind stress is defined as:

$$\tau_x = -c_m u_2 \tag{19}$$

Since T_{air} is a function of -1/L, it is also a function of $-u^{-3}$ which explains why the formulation for the air temperature blows up to large negative values when the wind speed decreases under very stable conditions.

In order to correct this, the calculation of the 2 m air temperature was switched in favor of a formulation that was not as dependent on the wind speed (Geleyn 1988). There are two formulations - stable and unstable. The stable case is presented first.

$$T_{air} = T_{sfc} + \frac{T_2 - T_{sfc}}{b_h}\left[\ln(1 + \frac{z}{z_2}(e^{b_n} - 1)) - \frac{z}{z_2}(b_n - b_h)\right] \tag{20}$$

The subscripts in the formula denote the value of the variable at that model level. The value of z is 2 m in this formula. Exchange coefficients for momentum and heat are incorporated into this formulation via the variables b_n and b_h. These are determined as follows:

$$b_n = \frac{k}{\sqrt{C_n}} \tag{21a}$$

$$b_h = \frac{k\sqrt{C_m}}{C_h} \tag{21b}$$

The constant k is von Kármán's constant (0.4), and C_n is the neutral exchange coefficient, defined as

$$C_n = \left[\frac{k}{\ln\frac{z_2 + z_0}{z_0}}\right]^2 \tag{22}$$

The unstable formulation is as follows:

$$T_{air} = T_{sfc} + \frac{T_2 - T_{sfc}}{b_h}\left[\ln 1\left(+\frac{z}{z_2}(e^{b_n} - 1)\right) - \ln\left(1 + \frac{z}{z_2}(e^{b_n - b_h} - 1)\right)\right] \tag{23}$$

The Geleyn formulation performs much better than does the Holtslag method (Fig. 16). Also note that with the new method of calculation, T_{air} is also more consistent with the values of the temperatures of the surface and the first model level, except around sunset when the boundary layer is changing from an unstable regime to a stable one. Under the old method, the value of the 2 m air temperature would often not be between the values of the surface and 20 m temperatures. While it is possible that the 2 m temperature not lie between the other 2 temperatures, it is unlikely.

Similarly, the same interpolations can be performed for calculating the 10 m wind speed, which is the typical surface observation level. The stable case would become

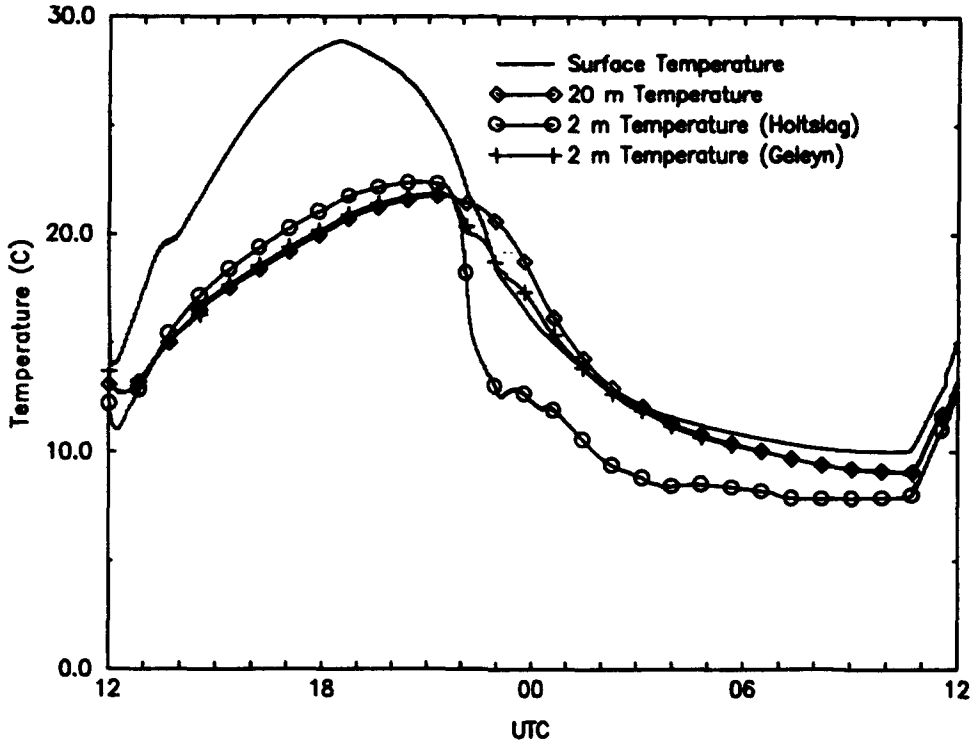

Fig. 16. A comparison of the Holtslag (1987) and Geleyn (1988) methods for diagnosing the 2 m temperature for the same composite 24 hour PBL model run. Surface and 20 m temperatures are included to show the validity of the two interpolation formulae.

$$U = \frac{U_2}{b_d}\left[\ln\left(1+\frac{z}{z_2}(e^{b_n}-1)\right)-\frac{z}{z_2}(b_n-b_d)\right] \tag{24}$$

where

$$b_d = \frac{k}{\sqrt{c_d}} \tag{25}$$

and the unstable case becomes

$$U = \frac{U_2}{b_2}\left[\ln 1+\left(\frac{z}{z_2}(e^{b_n}-1)\right)-\ln 1\left(+\frac{z}{z_2}(e^{b_n-b_d}-1)\right)\right] \tag{26}$$

Note that all of these formulations are interpolations using values of the variables at the surface and at the first model level.

2. Change in Boundary Layer Timestepping Scheme

It was discovered early in this study that there existed numerical instabilities in the model. These instabilities frequently occurred during the rapid growth of the PBL associated with maximum heating, or immediately after maximum growth had been achieved.

The numerical scheme in the boundary layer portion of the model consisted of a leap-frog scheme, and every 25 timesteps, a predictor-corrector scheme was used to try and damp any oscillations that may have been occurring. Unfortunately, some previous studies only looked at hourly output from the model and may have missed the oscillations that were occurring, or perhaps previous studies did not contain the large oscillations that appeared early on in this study.

In order to try and correct this deficiency in the model, the predictor-corrector scheme was called every third time step in an attempt to damp out the oscillations. The results were promising as the oscillations were significantly dampened (Fig. 17). Although this change in the numerical scheme did affect the results from the model, the effect was small (approximately 5% difference), and the results were felt to be more reliable due to the lack of oscillations in the model output.

However, the underlying numerical instability is still present in the PBL

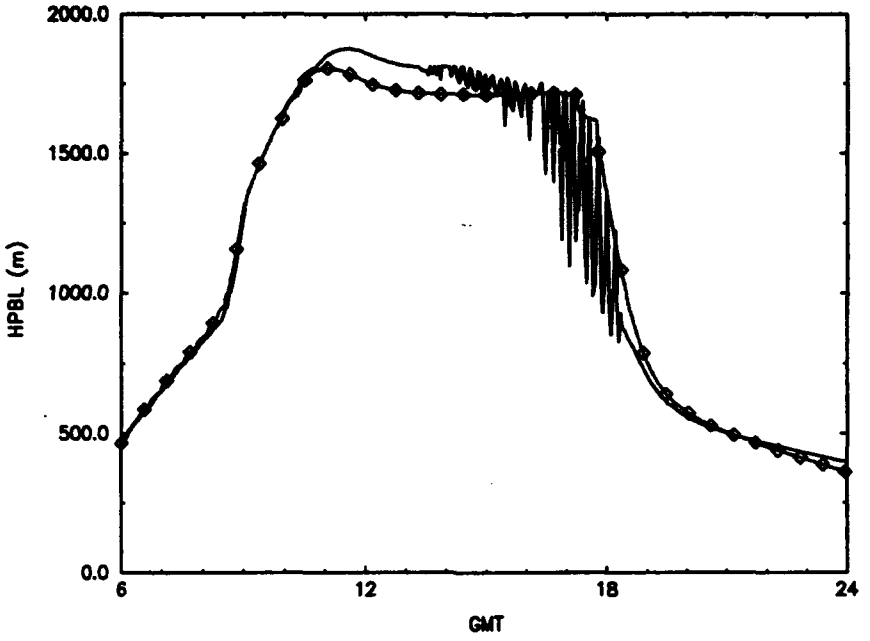

Fig. 17. Height of the PBL for a case during the Hydrological and Atmospheric Pilot EXperiment (HAPEX) experiment using two different numerical schemes. Solid, unmarked line is for scheme with the predictor-corrector step called every 25th timestep. Marked line is for scheme calling predictor-corrector step every 3rd timestep

model, and investigators at OSU are working on the problem (Ek, personal communication, 1994). A shorter time step was also attempted, but did not resolve the problem. A full numerical stability analysis was beyond the reach of this study.

3. Determination of PBL Height under very Stable Conditions

Another problem that appeared at the beginning of the minimum temperature study, and is somewhat related to the 2 m air temperature problem was the determination of the PBL height under extremely stable conditions. The model would diagnose a PBL height less than the height of the second model

level (~20 m), which would cause the model to fail. To correct this, a flag was placed in the model code that set the minimum PBL height under stable conditions to the maximum of the following three values: calculated PBL height, 50 m, or $0.07\frac{u^*}{|f|}$ where f is the Coriolis parameter (Koracin and Berkowicz 1988). This formulation led to a more realistic determination of the PBL height under extremely stable conditions. It should be noted that no oscillations in the PBL height were uncovered using this modification.

D. ADAPTATION OF THE OSU 1-D PBL MODEL AS AN AMT MODEL

In order to adapt the OSU model as an AMT model, the method of Holtslag *et al.* (1990) was followed. Some slight changes were needed due to the differences in the data received here at FSU, but the overall philosophy of the Royal Netherlands Meteorological Institute (KNMI) approach was adhered to.

1. Determination of Trajectories

In order to develop the AMT model, backwards trajectories in time needed to be determined. What this means is that for 3 levels - 975 hPa, 850 hPa, 700 hPa - trajectories needed to be determined that arrived at the forecast point at the forecast time at each of the above pressures. These trajectories are currently calculated by the National Meteorological Center (NMC) using a trajectory model based on the Nested Grid Model (NGM) data. This information

is then distributed in 8 different "FOUS" bulletins which contain information for different regions of the country. The bulletins contain trajectory locations in both the horizontal and vertical at 6 hour increments, arriving at the receptor point 24 hours after the start of the trajectory. Note that the bulletins give information for trajectories which arrive at a station at the surface, 850 hPa and 700 hPa. These trajectories can experience significant vertical motions during the forecast period.

It was mentioned above that the AMT model needs trajectory information for 975 hPa, 850 hPa and 700 hPa. It has been assumed in the AMT model that the surface trajectories are the trajectories for all air parcels arriving at the station from the surface up to 975 hPa. Since trajectory information is not received above 700 hPa, and more importantly, since the height of the PBL rarely, if ever, exceeds 700 hPa during return flow, it has been assumed that all trajectories above 700 hPa are equivalent to the 700 hPa trajectories. No important information is lost using this approximation since the primary focus of this study is the evolution of the PBL. Trajectories for all other levels are interpolated between the NGM forecast trajectories.

2. Determination of Input Sounding

The method for determining the input sounding was originally developed by Reiff *et al.* (1984) and was modified slightly by Holtslag *et al.* (1990). The modified procedure was used in this study with the additional modification of adding the horizontal and vertical wind components.

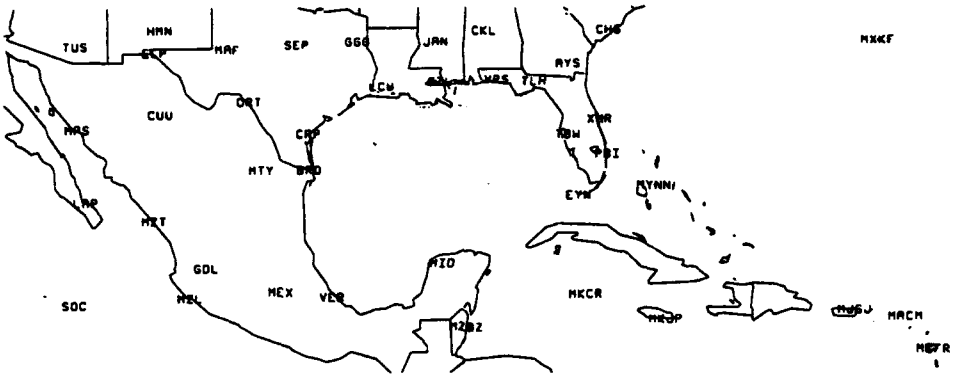

Fig. 18. Available radiosonde stations in the Gulf of Mexico region.

There exist numerous radiosonde stations in the Gulf region (Fig. 18). Not all of these stations, mainly the Mexican ones, report twice a day. In any event, all of the available soundings are processed by GEMPAK. Each of these soundings contain P, T, q, u and v for each significant level in the sounding.

To make the initial profile, all of the significant levels of the input soundings are used as significant levels for the analyzed sounding. The values of T, q, u and v for the analyzed sounding are obtained from the input soundings by using a weighting procedure on a given sigma level in the horizontal. The weights are inversely proportional to the square of the distance from each input sounding to the starting point of the trajectory at that sigma level.

Every significant level in the actual, input soundings are used in the analyzed profile. Since the accuracy of the analyzed profile can not be greater than that of the original soundings, the number of points must be reduced.

Following Holtslag *et al.* (1990), if adjacent levels in the profile differ by less than 3 hPa , 0.3 K and 0.2 g kg^{-1}, then only the lowest level is kept. Also, if a level is within the same tolerances for T and q from the interpolated value at that level using adjacent upper and lower levels, then that level is not used in the analyzed sounding. This analyzed sounding is then interpolated onto the above-mentioned PBL model grid using a least squares method.

Unfortunately, this method does not work very well over water after a cold front has passed through the region. The first few days after cold-frontal passage, before the return flow has reached a maximum, the skies are typically clear, and radiation inversions tend to set up at night. Thus many of the 1200 UTC soundings that surround the Gulf of Mexico contain this radiation inversion which then appears in the analyzed sounding. For example, the trajectories arriving at Mobile, AL, (MOB) on 27 January 1994 at 1200 UTC originate 24 hours earlier in the eastern Gulf of Mexico (Fig. 19). The resultant analyzed sounding derived from the above method is much too dry, and contains a

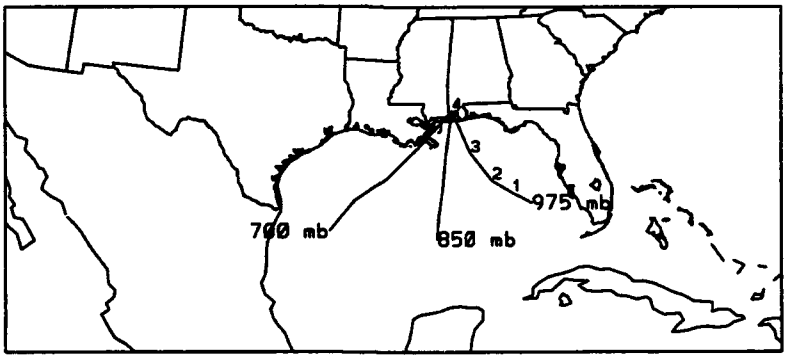

Fig. 19. Twenty-four hour back trajectories arriving at MOB at 1200 UTC, 27 January 1994. Pressures indicate pressure at which the trajectory arrives. Six-hourly positions of the low-level trajectory are indicated.

temperature inversion: the lowest part of the sounding is heavily influenced by the actual sounding taken at Tampa, FL, (TBW) since that is the closest radiosonde site to the starting point of the 975 hPa trajectory (Fig. 20). This inversion is very unrealistic over the middle of the Gulf of Mexico. Regardless of the source region of the air, modification of the airmass will have taken place as it tracked over the Gulf which will have wiped out the radiation inversion.

Several dropsondes from February 1994, were analyzed which reinforced the above statement. A majority of these dropsondes took place near the middle of the Gulf of Mexico and did not exhibit the radiation inversion that the analyzed soundings almost always exhibited (Fig. 21). A typical sounding from one of the dropsondes contained a slightly superadiabatic layer in the lowest 30 hPa, followed by an approximately adiabatic lapse rate until a subsidence inversion is reached. The air is almost completely saturated up to the subsidence inversion. The low-level temperature profiles from the dropsondes is vastly different than the radiation inversion that was normally found in the analyzed sounding using the above weighting method.

Also, during GUFMEX, several ships were in the Gulf of Mexico which launched frequent radiosondes. Lewis and Crisp (1992) show the thermodynamic profiles taken by a ship as it moved southward in the Gulf, immediately after a cold-frontal passage, and as it moved northward in the Gulf, after the return flow had started. For the cold front case, the soundings showed a temperature profile with a superadiabatic lapse rate in the lowest part of the atmosphere, followed by a layer which is more adiabatic up to a subsidence

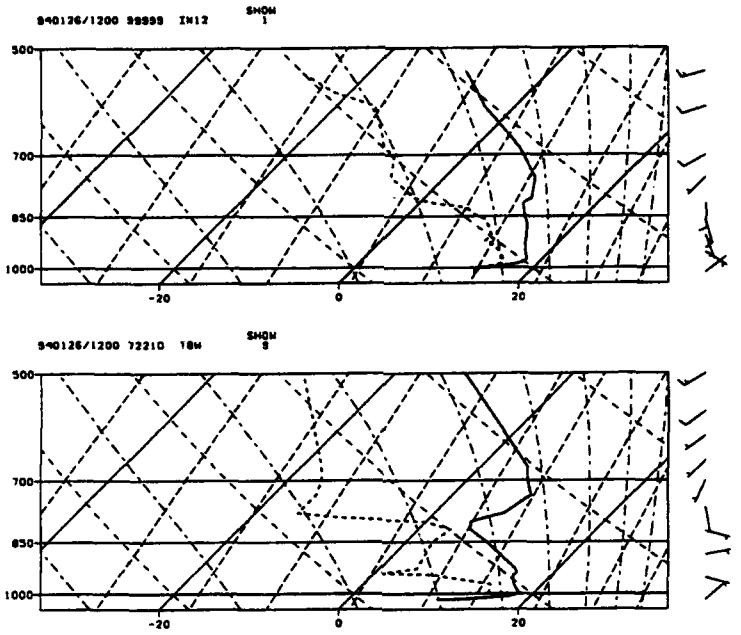

Fig. 20. Input sounding derived for trajectories shown in Fig. 19 for 1200 UTC, 26 January 1994 (top). Tampa, FL, sounding for same time (bottom)

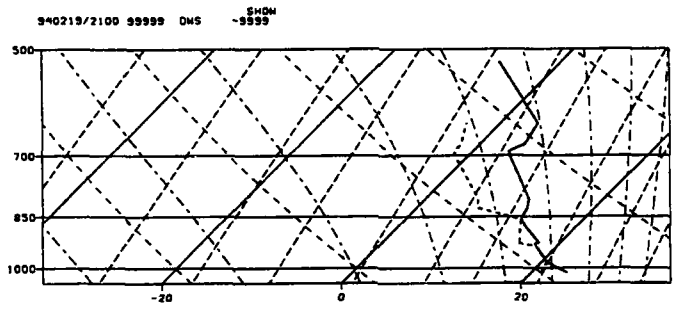

Fig. 21. Skew-t from dropwinsonde at 2100 UTC, 19 February 1994. Location of the drop was 26.6 °N, 87.5 °W.

inversion. The soundings became increasingly warm and moist as the ship moved farther south, indicating the transformation of the air mass as it moved over the warm water of the Gulf. Also, the subsidence inversion aloft became more pronounced with time.

Similar results occurred when the soundings were taken coincident with the return-flow. A shallow, super-adiabatic lapse rate occurred at the surface, followed by an adiabatic lapse rate, up to a subsidence inversion. Moisture tended to be well mixed above the super-adiabatic level, and below the subsidence inversion, with almost constant dew points in this region.

3. Land-sea Mask

In order for the surface fluxes to be calculated correctly, it is important to determine whether the AMT model is over land or water as it is advected along the low-level trajectory. It was determined that with a time step of 3 minutes, a resolution of 0.1 degree would be accurate enough to show details in the coastline in the return-flow region. A land-sea mask was then formed and read into the model (Fig. 22). Most of the details of the coastline are well-represented by the mask and are more than adequate for determining whether the lowest trajectory is over land or water.

4. Sea Surface Temperatures

Sea surface temperatures (SSTs) were needed as a prescribed bottom-

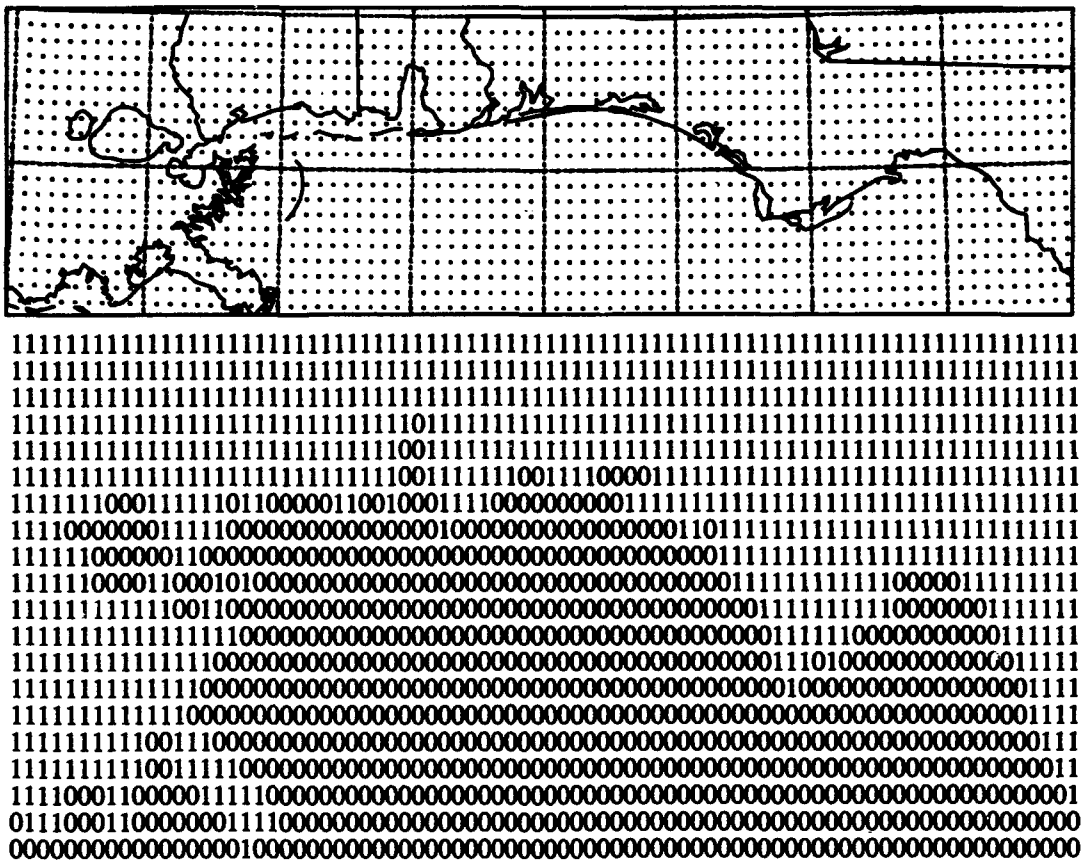

Fig. 22. The Gulf Coast from 83-91 °W and 29-31 °N (top). The dots indicate 0.1 degrees. Matching land-sea mask at 0.1 degree resolution (bottom).

boundary condition when the model was determined to be over water. SSTs were acquired from an anonymous file transfer protocol (FTP) site at National Oceanic and Atmospheric Administration (NOAA)[1]. These data are a combination of in-situ measurements and satellite-derived observations. A complete description of the analysis procedure is given in Reynolds and Smith (1993).

The analysis is produced weekly on a one degree grid. However, before

[1] Internet address is nic.fb4.noaa.gov

the analysis is computed, the satellite-derived data is adjusted for biases as described in Reynolds (1988) and Reynolds and Marsico (1993). Although this bias correction does improve the accuracy of the analysis, it does add a small amount of noise in time. Thus, NOAA recommends that a binomial filter in time, 1/4-1/2-1/4, be used to eliminate the noise.

After smoothing the data, the data was interpolated to the same 0.1 degree grid as the land-sea mask using a 4-point interpolation routine obtained from Prof. T Krishnamurti at Florida State University (personal communication, 1993).

5. Forecast of Horizontal Wind Components

In order to properly forecast u and v at every time step, it was felt necessary to include both turbulent processes and large-scale synoptic processes. Although the PBL model does incorporate turbulent and large-scale processes in the prognosis of u and v, its treatment of the large scale processes is not robust enough due to the neglect of advection.

Currently, the prognostic equation for u and v is given by (11a). In the model, which uses a semi-implicit scheme, this is "coded" as

$$\frac{u^+ - u^-}{\Delta t} = fv^0 + \frac{\partial}{\partial z}\left(K_m \frac{\partial u^+}{\partial z}\right) + w\left(\frac{\partial u^-}{\partial z}\right) \qquad (27)$$

for the u-component of the wind. The plus, minus or zero subscript refer to the next value, previous value, and current value of the wind, respectively. A similar

equation exists for the v-component, with the appropriate sign change for the Coriolis term.

Since this is a 1-d model, missing from the above equations is the pressure tendency term, since no information is known about the horizontal pressure gradients. However, in the AMT model, horizontal processes play an important role. The problem is that the model is still effectively a 1-d model which is being advected along a horizontal trajectory. In order to take into account the large scale horizontal processes that are playing a role in the determination of the u and v fields, information about these fields from the NGM is incorporated into the model.

Information about the large-scale, forecast u and v fields are received from NGM output at the 6 hourly locations of the three trajectories. These fields are then interpolated at every time step in vertical and horizontal space in the model as are the trajectory locations. These values are then incorporated into the model in the following manner: equation (27) can be written as

$$u^{+} = u^{-} + diff(u) + \text{vertical advection}(u) \qquad (28)$$

with forecast values for u and v used as u^{-} in the above equation. The values for u and v from the previous time step are then used to determine the vertical diffusion and advection portions of the above equation. Each of these is then added to get the new value for u at that time step. Thus, both turbulent and large scale processes are incorporated into the forecasts for u and v. Above the PBL, where turbulence is negligible, the u and v components are set equal to the

forecast winds from the NGM.

6. Determination of Pressure

As the model moves along the lowest trajectory, the surface pressure can be expected to change. Calculation of the surface pressure is done by simply interpolating in time between the starting pressure and the ending pressure. The starting and ending surface pressures are also retrieved from the NGM output for the origin and end of the low-level trajectory.

The value of pressure at the other model levels is then adjusted to take into account the vertical motion of the trajectories as well as the new value of the surface pressure. Since the air mass may have undergone vertical contraction or expansion, the height field is recalculated using a hydrostatic integration.

7. Calculation of 2 m Temperature and 10 m Wind Speed

The adoption of the Geleyn (1988) formulation for the calculation of both the 2 m temperature and 10 m wind speed was discussed earlier in the section on changes to the OSU model. Unfortunately, this formulation does not seem to work well over water (Fig. 23) The low level trajectory was over water for the first 23 hours of the 24-hour model run. As can be seen, the formulation adopted from Geleyn (1988) does not provide a very realistic diagnosis of the 2 m temperature - with both the 20 m and surface temperatures much above the 2 m temperature, or the 10 m wind speed - with the 20 m wind speed being

significantly lower than the 10 m wind speed.

The reason for this failure is not too easily explained. Over water, surface roughness is dependent on the wave heights which is dependent on the wind speed. Typical roughness lengths over the water tend to be on the order of $3x10^{-5}$ m. The neutral exchange coefficient, C_n, is dependent on the roughness length, z_0 (22). Values for C_n are approximately $5x10^{-3}$ over land and an order of magnitude less over water. It would appear that the Geleyn interpolation formulae do not provide realistic results when the values for the neutral exchange coefficient are too low.

Based on this result, the discussion regarding dropsondes and the Lewis and Crisp paper, a simple linear interpolation between the surface and the first model level has been adopted for calculating the 2 m air temperature when the model is determined to be over water. The old method for calculating the 10 m wind speed has also been adopted for when the model is over water as it did not suffer the same inadequacies as the original 2 m temperature formulation.

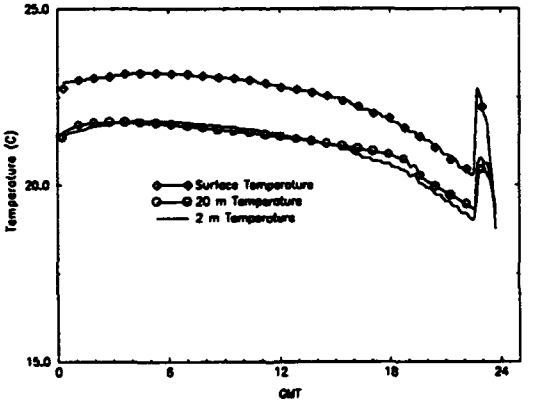

Fig. 23. Temperatures for AMT run arriving at (BRO) at 00 UTC, 19 February 1994. Steplike appearance of temperatures is due to the resolution of the SST field.

CHAPTER 3. MINIMUM TEMPERATURE STUDY

A. Introduction

Alluded to earlier was the fact that TLH often has the lowest minimum temperature in the southeastern United States 1-2 days after passage of a cold front (Fig. 24). Fuelberg and Elsner (personal communication, 1994) have tried to show that this is due mainly to radiational cooling, and not cold air drainage - a popular public opinion. The PBL model was used in conjunction with their study in order to strengthen their conclusions. Also, this study helped to further test the new 2 m temperature scheme. The results of this minimum temperature study are presented first, followed by a look at several of the individual cases in order to see under what circumstances the model performed well and under what circumstances the model performed poorly.

B. Data Gathering

Data for all the days in 1993 that Fuelberg and Elsner studied (days where good radiational cooling was felt to have occurred) were obtained for this study. The data included minimum temperatures for 12 locations around TLH, as well as the official minimum temperature recorded at TLH. Winds and sky conditions were available at 3 hourly increments for each of the nights

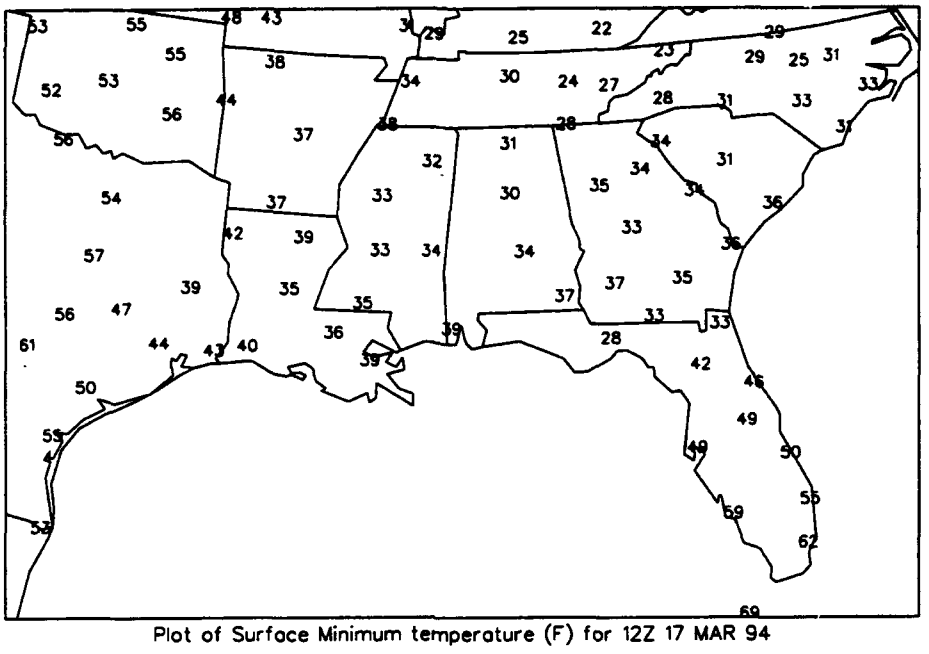

Fig. 24. Minimum temperatures for the southeastern United States for 17 March 1994.

concerned. From this dataset, 12 nights were selected based on 2 criteria which were important for the development of strong radiational cooling - clear skies, and winds less than 5 kt for at least 6 hours before the minimum temperature occurred. It was felt that the PBL model would perform best under these conditions. During this selection process, no effort was made to look at the large scale flow to determine if advection would be an important factor, as it was felt the criterion of light winds would preclude this possibility. Four other nights from Fall, 1993, which were not part if the original study, have also been included in the study to increase the sample size. The above criteria were followed for the selection of these cases as well.

C. Model Performance

Twelve and 24-hour runs of the model were made for each of the 16 days selected. The method of determining input soil moisture discussed in chapter 2 was used (Table 1). Minimum temperatures forecasted by the PBL model were compared to 12 and 24-hour runs for the Limited Fine Mesh model (LFM) and the NGM as well persistence and climatology (Table 2). Low level temperature advection, averaged between the surface and 700 hPa, was also calculated

Table 1. Soil moistures used to initialize the various PBL model forecasts in the minimum temperature study. Percentages indicate percent of saturation.

	24HR Forecast	12 HR Forecast
16Feb93	30%	30%
20Feb93	30%	25%
9Mar93		30%
30Mar93	30%	30%
7Apr93	30%	30%
12Apr93	30%	30%
19Apr93	30%	
20Apr93		30%
23Apr93	20%	20%
24Apr93	20%	20%
25Apr93	20%	20%
29Apr93	30%	30%
1Oct93	30%	30%
24Nov93	30%	30%
29Nov93	30%	30%
30Nov93	30%	30%

Table 2. Temperature data for TLH for the 16 days in the minimum temperature study. Included are the observed minimum temperatures for the day (OBS) as well as 12 and 24-hour forecasts from the PBL, LFM and NGM models. Also included are persistence and climatology. Temperature advection (Tadv, °F/day) at 1200 UTC for each day is also included. Parentheses indicate the difference between the observed value and the forecast value.

DATE	OBS	24HR PBL	12HR PBL	24HR LFM	12HR LFM	24HR NGM	12HR NGM	Prstnce	Climo	Tadv 1200 UTC
16Feb93	45	37(-8)	34(-11)	49(+4)	49(+4)	52(+7)	51(+6)	39(-6)	44(-1)	16.3
20Feb93	27	13(-14)	20(-7)	32(+5)	38(+11)	27(0)	33(+6)	27(0)	42(+15)	4.1
9Mar93	40		41(+1)	41(+1)	44(+3)	41(+1)	47(+7)	39(-1)	43(+3)	-2.7
30Mar93	49	47(-2)	55(+6)	51(+2)	55(+6)	48(-1)	57(+8)	48(-1)	52(+3)	3.1
7Apr93	43	45(+2)	46(+3)	46(+3)	47(+4)	47(+4)	48(+5)	50(+7)	47(+4)	-1.6
12Apr93	43	42(-1)	50(+7)	49(+6)	52(+9)	50(+7)	51(+8)	43(0)	51(+8)	
19Apr93	41	46(+5)		47(+6)	45(+4)	42(+1)	45(+4)	47(+6)	53(+12)	
20Apr93	45		43(-2)	49(+4)	49(+4)	50(+5)	50(+5)	41(-4)	54(+9)	0.9
23Apr93	31	28(-3)	31(0)	35(+4)	36(+5)	32(+1)	33(+2)	36(+5)	58(+27)	0.5
24Apr93	35	26(-9)	36(+1)	45(+10)	45(+10)	41(+6)	42(+7)	31(-4)	55(+20)	3.4
25Apr93	51	32(-19)	49(-2)	55(+4)	58(+7)	56(+5)	59(+8)	35(-16)	53(+2)	4.7
29Apr93	41	43(+2)	45(+4)	47(+6)	47(+6)	43(+2)	48(+7)	45(+4)	55(+14)	-0.5
1Oct93	42	42(0)	44(+2)	44(+2)		44(+2)	43(+1)	50(+8)	62(+20)	-3.1
24Nov93	45	45(0)	46(+1)	47(+2)		48(+3)	48(+3)	47(+2)	45(0)	-2.9
29Nov93	29	30(+1)	31(+2)	31(+2)		31(+2)	31(+2)	38(+9)	44(+15)	-6.3
30Nov93	32	30(-2)	33(+1)	31(-1)		35(+3)	33(+1)	29(-3)	44(+12)	-2.0

using GEMPAK in order to determine if temperature advection could account for any discrepancies between the PBL model forecasted minimum temperatures and the actual minimum temperatures. Missing values for the PBL runs indicates that data (input soundings) were not available to initialize the model for those days; similarly, missing values for temperature advection indicate that GEMPAK data were not available for the calculation of temperature advection. In May, 1993, NMC stopped providing 12 hour minimum temperature forecasts from the LFM which accounts for the missing values for the latter days.

Scatter plots were done in order to try and assess how well each different forecast category performed (Fig. 25). Correlation coefficients were also calculated in order to perform a more objective analysis (Table 3). The large scale models' forecasts of the minimum temperature were more correlated than were the PBL model's forecasts of the minimum temperature. All 4 of the large scale model forecasts had a correlation coefficient of around 0.95, while the PBL model showed increasing skill as projection time decreased; correlation coefficients ranged from 0.74 (24-hour forecast) to 0.87 (12-hour forecast). Climatology and persistence were less correlated than were any of the models due to the nature of the study.

The above results, while somewhat encouraging, are certainly not robust

Table 3. Correlation coefficients (r) for each forecast category vs. observed.

	12hr LFM	24hr LFM	12hr NGM	24hr NGM	12hr PBL	24hr PBL	Prstnce	Climo
r	0.93	0.94	0.97	0.96	0.87	0.74	0.61	0.25

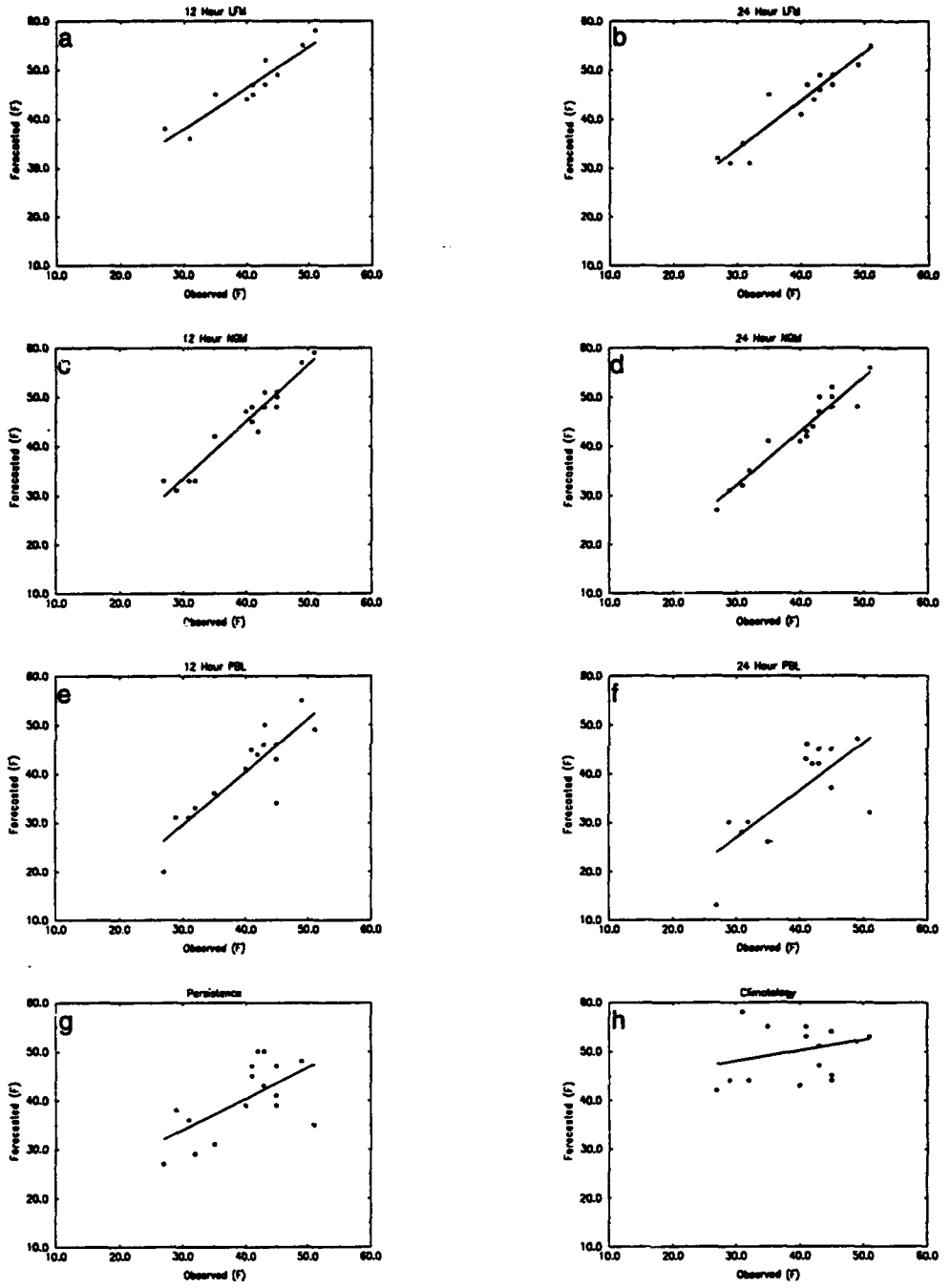

Fig. 25. Scatter plots for forecasts of minimum temperature vs. observed minimum temperature for each of the forecast categories. Solid line indicates linear regression fit to the data. Shown are forecasts from (a) 12-hour LFM, (b) 24-hour LFM, (c) 12-hour NGM, (d) 24-hour NGM, (e) 12-hour PBL, (f) 24-hour PBL, (g) climatology, and (h) persistence. Correlation coefficients are shown in table 3.

enough to make any statement regarding the usefulness of the PBL model for forecasting minimum temperatures as the model does not appear to be more skillful than either of the statistical guidance products available. However, additional statistics were calculated in order to more thoroughly compare the PBL model with the LFM, NGM, persistence and climatology. These statistics were as follows (Table 4): (1) bias; (2) percent of cases a model forecast was too warm and (3) the corresponding average difference; (4) percent of cases a model forecast was too cold and (5) the corresponding average difference; and (6) percent of cases that a model correctly forecasted the minimum temperature.

These results were more encouraging with respect to the PBL model.

Table 4. Various other statistics calculated for each forecast category. Average differences between forecast and actual minimum temperatures are expressed in °F.

	12hr LFM	24hr LFM	12hr NGM	24hr NGM	12hr PBL	24hr PBL	Prstnce	Climo
Bias	7.15	3.75	5.00	3.00	0.33	-3.42	0.38	10.19
% Greater than Observed	100	94	100	88	71	29	44	88
Avg Diff when Greater then Observed (°F)	6.2	4.1	5.0	3.5	2.8	2.5	5.9	11.7
% Less than Observed	0	6	0	4	22	57	44	6
Avg Diff when Less than Observed (°F)	---	1.0	---	1.0	5.5	7.3	5.0	1.0
% Within 2 °F of Observed	0	38	25	50	60	57	31	19

The 12-hour PBL forecasts contained only a slight warm bias, especially compared to the LFM and NGM. In fact, only once was either the LFM or NGM too cold in its forecast. The 24-hour PBL model runs showed an approximate 3.5 degree cold bias, the only category that did contain a cold bias. Possible reasons for this will be discussed later in this chapter.

For both 12 and 24-hour forecasts, when the forecast was higher than the observed minimum temperature, the PBL model performed better than either of the two large scale models and also better than persistence and climatology. Both PBL forecasts also had the largest number of forecasts within 2 °F of the observed minimum temperatures. As expected, the model performed best on days where there was little synoptic forcing, i. e. temperature and moisture advection were minimal.

The PBL model did not perform as well when the observed minimum temperature was warmer than the forecasted temperature, although there are very few cases available to compare the PBL model with the LFM or NGM. Several of the discrepancies can be explained by warm advection that was occurring on that particular day. These will be discussed in more detail in the next section.

D. CASE STUDIES

1. 16 February 1993

One of the days that the PBL model overestimated the amount of nocturnal cooling was 16 February 1993. At 1200 UTC on the 16th, significant

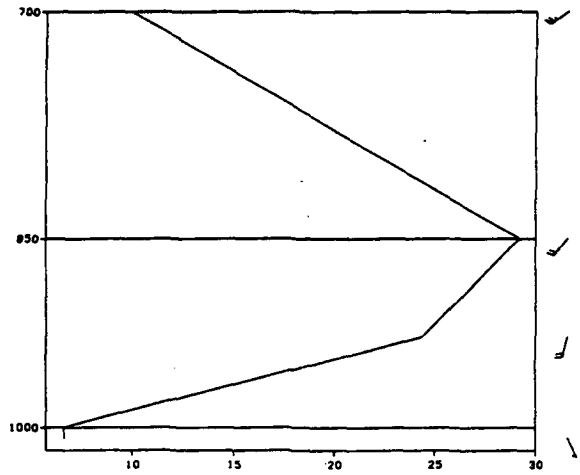

Fig. 26. Temperature advection (°F/s x 10^5) from the surface to 700 hPa at 1200 UTC, 16 February 1993 at TLH.

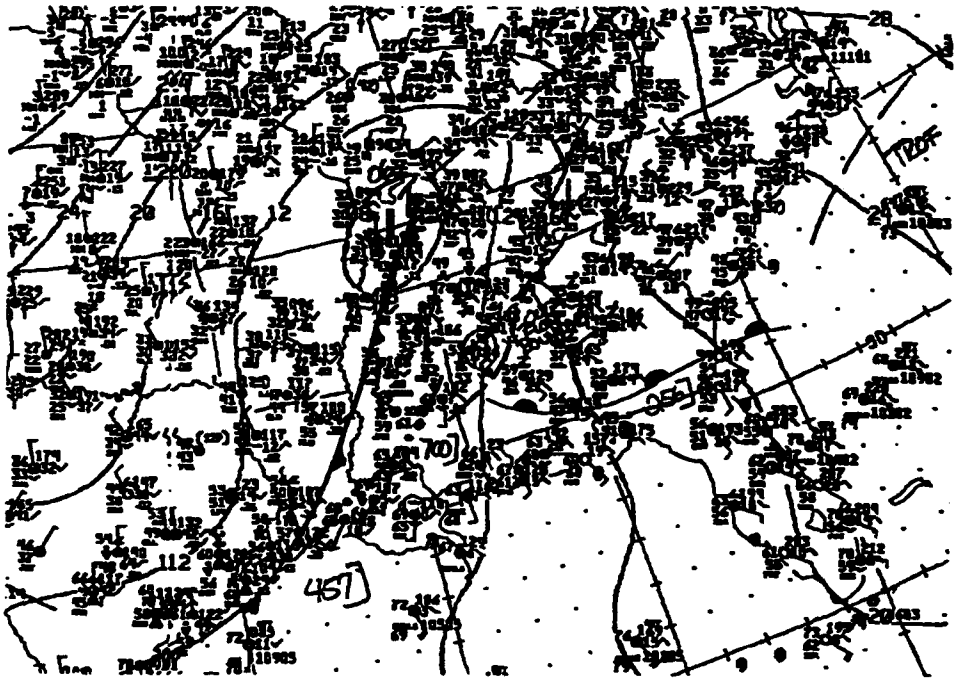

Fig. 27. NMC surface analysis for 0600 UTC, 16 February 1993.

warm air advection was occurring from the surface to 700 hPa on the order of 10 °F/day (Fig. 26). The large-scale synoptic flow was out of the south, and a warm front was just north of TLH at 0600 UTC on the 16th (Fig. 27). In fact the minimum temperature of 45 °F occurred at 0550 UTC, after which temperatures began to rise.

The PBL model was too cold in its forecast for the following reason: the warm front passed through TLH between 0000 UTC and 0600 UTC on the 16th. Both the 24 and 12-hour model forecasts were initialized from soundings taken when the surface warm front was to the south of TLH. Thus the air mass that was present at TLH at 1200 UTC on the 16th, was not the same air mass that initialized the model 12 and 24 hours earlier. Since the model does not contain horizontal advection and other large scale forcing, it could not forecast the change in the airmass, and continued to decrease the temperature all night.

2. 25 April 1993

A similar situation to 16 February occurred on 25 April 1993. A warm front was analyzed to the southwest of TLH at 1200 UTC on 24 April (Fig. 28). Dewpoints were in the 50s and 60s south of the warm front, while north of the front, dewpoints were in the 40s and 50s. Although the front is not shown on subsequent surface analyses, dewpoints increased 10-15 °F along the eastern Gulf coast by 0600 UTC on 25 April (Fig. 29). The diffuse front seemed to have passed through TLH between 1200 UTC on the 24th and 00 UTC on the 25th, based on a slow increase in dewpoints and a gradual windshift.

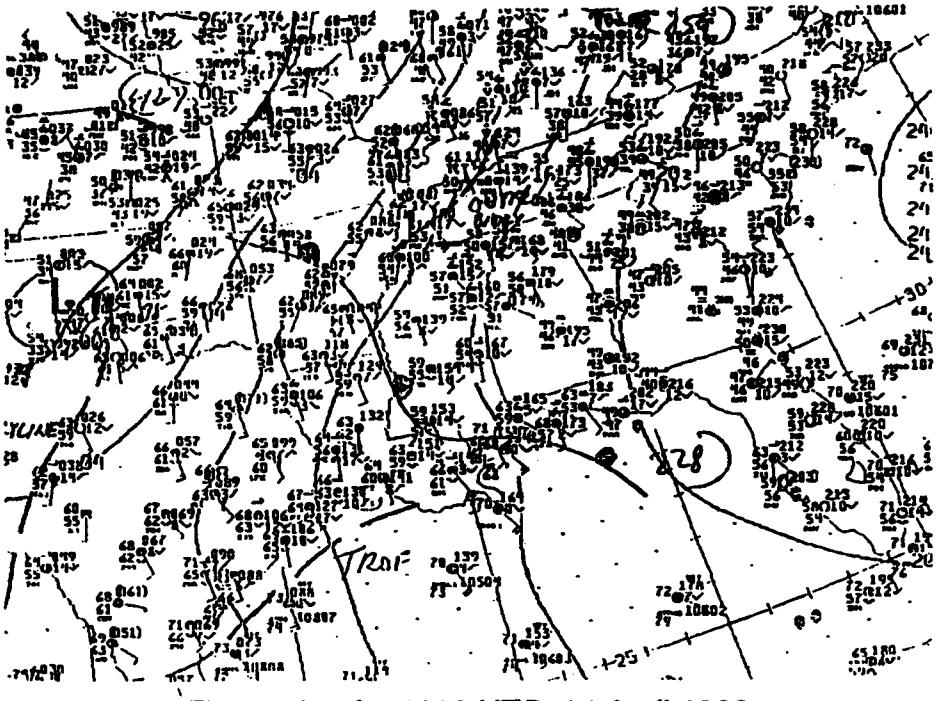

Fig. 28. As in Fig. 27, but for 1200 UTC, 24 April 1993.

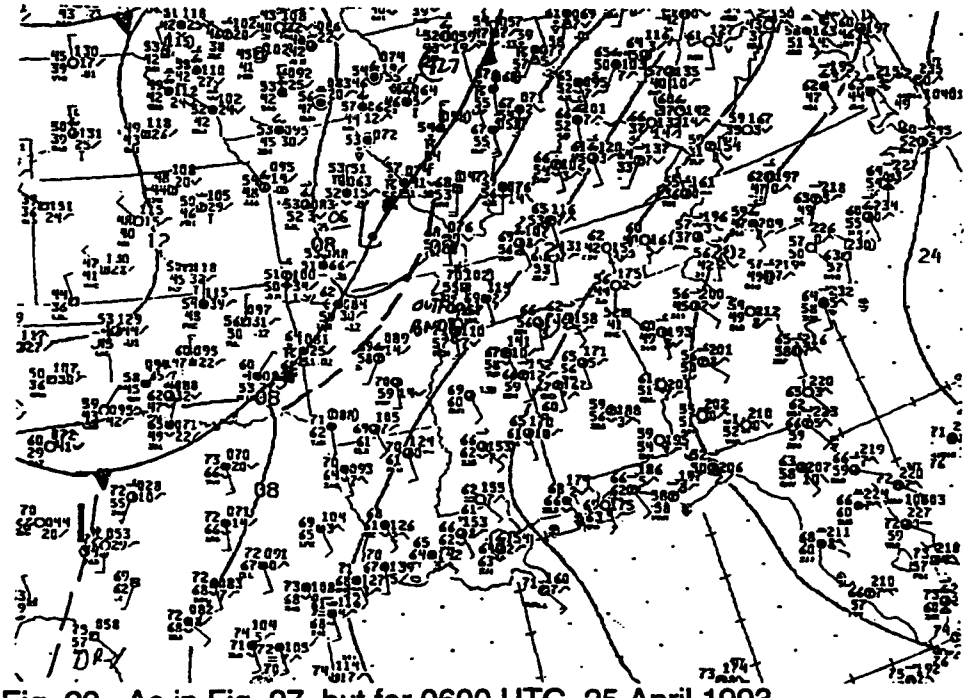

Fig. 29. As in Fig. 27, but for 0600 UTC, 25 April 1993.

The 24-hour PBL model forecast was too cold by 19 °F, while the 12-hour PBL forecast was only 2 °F too cold. This discrepancy is easily explained taking into account the surface analyses. What clearly occurred was that the 24-hour PBL model forecast was initialized within a cool, dry air mass which allowed good radiational cooling to occur in the model, in turn allowing the temperature to decrease rapidly after sunset. The 12-hour PBL model forecast was initialized with the warmer, moister air mass, which was not as conducive for radiational cooling in the PBL model. Thus the temperatures did not decrease as rapidly after sunset in the model.

3. 20 February 1993

The PBL model had a difficult time forecasting the minimum temperature on this day. Both the 24-hour forecast (14 °F too cool) and the 12-hour forecast (7 °F too cool) were the second worst forecasts for each category. It should be noted that the LFM also had a difficult time forecasting this day, especially the 12-hour forecast. Reasons for the PBL model failure are not readily apparent. Temperature advection was minimal during this period (2.3 °F/day) and clearly can not account for the 14 °F error in the 24-hour PBL forecast.

Although warm advection can probably be ruled out as the reason for the PBL model failure, moisture advection may have been the cause. Dewpoints between the surface and 700 hPa increased 10-20 °F between 1200 UTC on the 19th and 1200 UTC on the 20th (Fig. 30). A northeasterly flow had developed over the eastern panhandle of Florida as a high pressure system moved east off

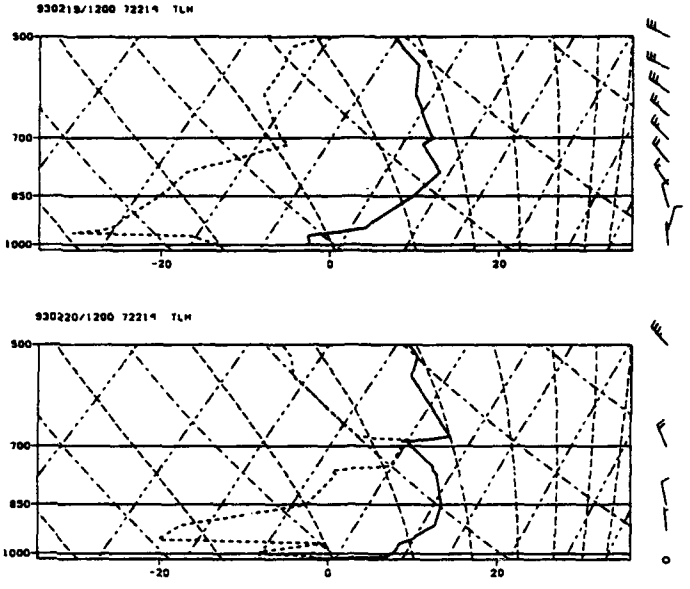

Fig. 30. Soundings from TLH for 1200 UTC, 19 February 1993 and 1200 UTC, 20 February 1993.

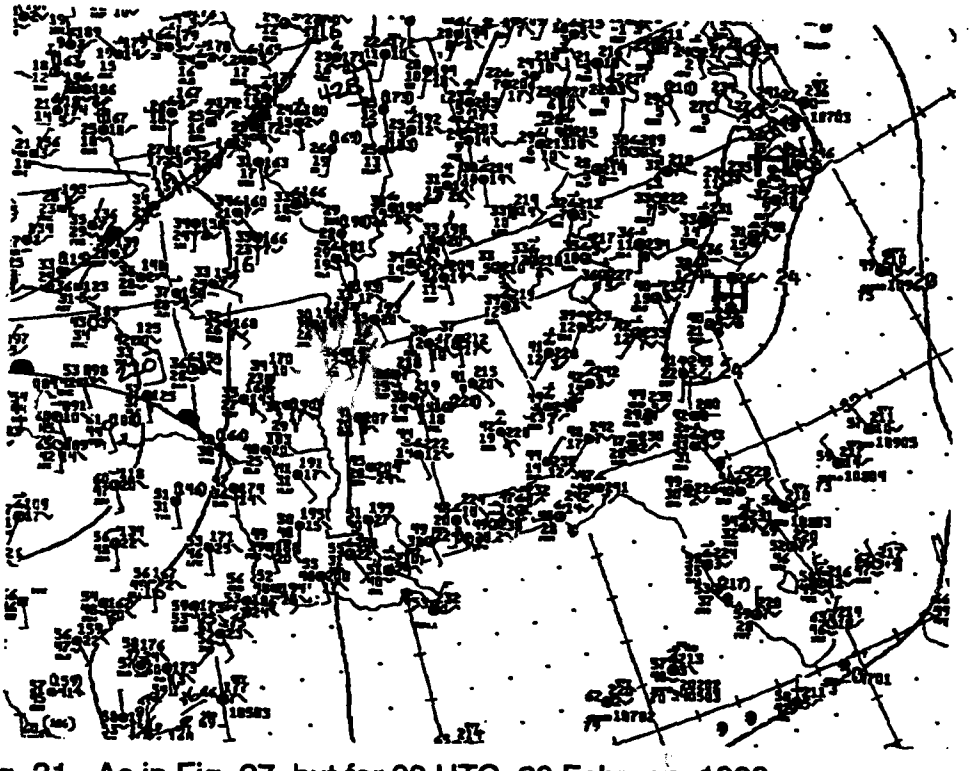

Fig. 31. As in Fig. 27, but for 00 UTC, 20 February 1993

the coast of the Carolinas (Fig. 31). This flow advected moisture from the Atlantic Ocean into north Florida.

Both of the PBL forecasts were initialized in a drier air mass than the one that existed when the minimum temperature occurred, thus the large discrepancies between the forecasted and the observed temperatures. With the drier conditions, conditions more conducive to radiational cooling could develop in the model, causing the model to seriously overpredict the amount of cooling that actually did occur. The 12-hour forecast was initialized in a slightly moister boundary layer, which explains why it did not as seriously overpredict the cooling which took place as the 24-hour forecast did.

4. 1 October 1993

As was discussed in section C, the model performed extremely well under conditions of light synoptic forcing, such as what occurred early in the fall of 1993. An unseasonably cool air mass moved into the southeastern United States on 30 September 1993. By 0000 UTC on 1 October 1993, dewpoints throughout the Southeast were in the 30s and 40s as the surface ridge line moved into the region (Fig. 32). These were ideal conditions for using the PBL model, which is why the sensitivity studies shown in chapter 2 were performed on this day.

The model did indeed perform well as the 24-hour forecast correctly predicted the minimum temperature, and the 12-hour forecast was only 2 °F too warm. Low-level cold advection, calculated at 1200 UTC 1 October 1993, was

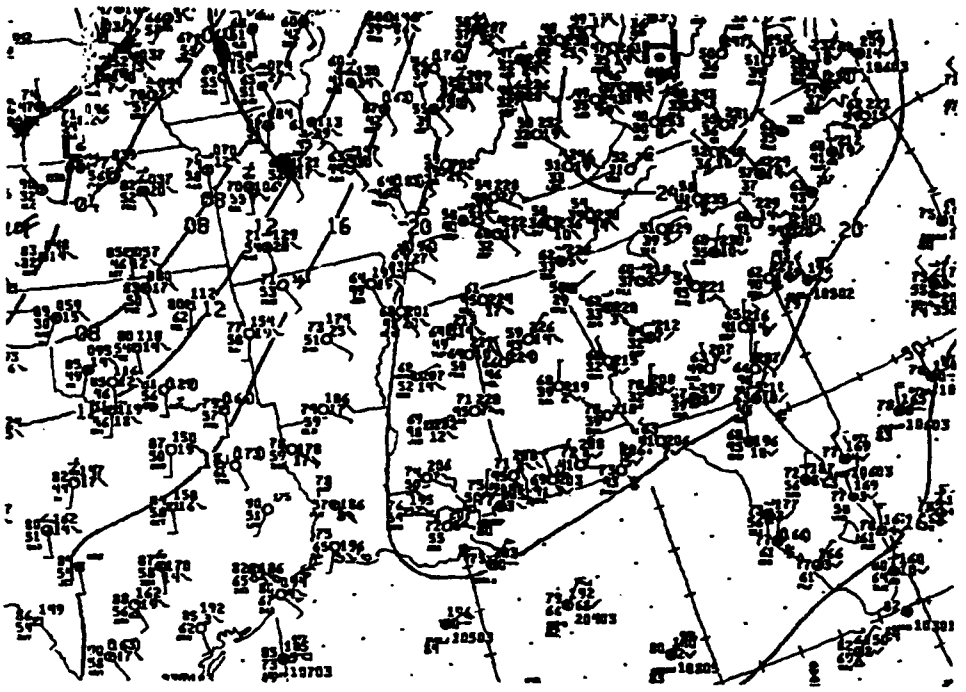

Fig. 32. As in Fig. 27, but for 00 UTC, 1 October 1993.

less than 2 °F/day. As an aside, the PBL model run initialized at 1200 UTC on 30 September 1993 was only 1 °F too cool in its prediction of the high temperature on that day (81 °F), and the 00 UTC 1 October run correctly predicted the high temperature for 1 October (83 °F).

E. MINIMUM TEMPERATURE STUDY CONCLUSIONS

Although the PBL model's forecasts of the minimum temperature at TLH were less correlated than were either of the large scale models, the 12-hour PBL forecast contained much less of a bias than either of the large scale models, and the 24-hour PBL's bias was similar in magnitude to the large scale models, but

opposite in sign. However, if the days discussed earlier in this chapter, where advection was shown to be the cause of the model's failure, are neglected in the calculation of the statistics, the PBL model's performance improves markedly. For the 12-hour PBL forecast, the correlation coefficient increases to 0.94, although the bias does increase slightly to 1.8 °F; for the 24-hour PBL forecast, the correlation coefficient jumps to 0.91, and the bias also improves, to -0.6 °F. The correlation coefficients for the PBL model compare with both of the large scale models, but the PBL model biases are much lower than either the LFM or NGM. It should be noted that when the statistics are recalculated for persistence, neglecting the same days as for the PBL model, the correlation coefficient increases to 0.75; however, the bias increases to 2.2 °F. Thus, even considering only synoptically quiet days, the forecasts from the PBL model are still better than those derived from persistence.

Looking at these statistics, it is clear that the PBL model can be a useful tool in forecasting minimum (and maximum) temperatures at a site similar to TLH, where good radiational cooling can develop. However, it is also clear that recognition of the PBL model's shortcomings during periods of large scale forcing is a must, in order to use this tool effectively. Blind use of the PBL model, without regard to the overall synoptic situation, can lead to significant forecast errors, as was seen earlier in this chapter. However, use of the PBL model, with its surface energy balance and crude radiative parametrization package, during periods of negligible synoptic forcing can be valuable to a forecaster in predicting daily temperature extremes.

CHAPTER 4. AIR MASS TRANSFORMATION MODEL RESULTS

A. Introduction

The synoptic situation that occurred in the Gulf of Mexico from 17 February - 23 February 1994, provided a good opportunity for testing the newly developed Florida State University air mass transformation (FSUAMT) model. In order to be able to objectively compare model output with actual soundings, only stations that launched rawinsondes and were included in the trajectory bulletins were used in this study. Unfortunately, this limited the number of cases that could be included as there are only two stations along the Gulf Coast that meet these criteria - BRO and TLH. However, trajectory information is available for New Orleans, LA (MSY), while soundings are performed at Slidell, LA (SIL) which is 40 miles northeast of MSY. In order to add another station to the study, the trajectories which arrived at MSY were adjusted to arrive at SIL. With only 3 cities, however, only eleven 24 hour model runs were able to be performed. Two more cases were added from a return flow event from 26 January - 27 January 1994 to increase the sample size.

A brief overview of the synoptic situation during the February return flow event will be presented first. Then model performance will be evaluated by looking at various statistics that were calculated in order to compare the model-derived thermodynamic profiles with the actual thermodynamic profiles. Lastly,

some specific cases will be presented to more subjectively look at model performance.

B. Synoptic Situation for 16 February - 23 February 1994

A cold front swept through the Gulf Coast region on 15 February 1994, and by 1200 UTC on the 17th, the low level flow from the Gulf of Mexico was arriving at BRO (Fig. 33). As the high pressure system tracked east, the flow became more southerly along the Texas coast, and return flow began along the Louisiana coast around 00 UTC on the 19th (Fig 34).

By 1200 UTC on the 23rd, the return flow had stopped along the Texas

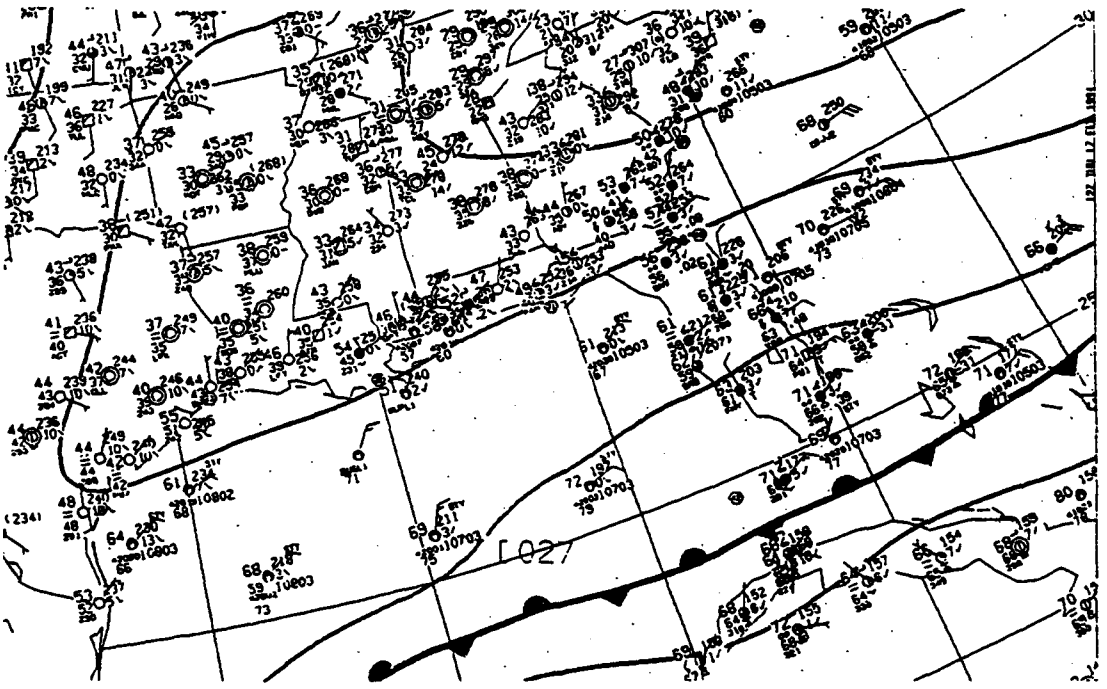

Fig. 33. As in Fig. 27, but for 1200 UTC, 17 February 1994.

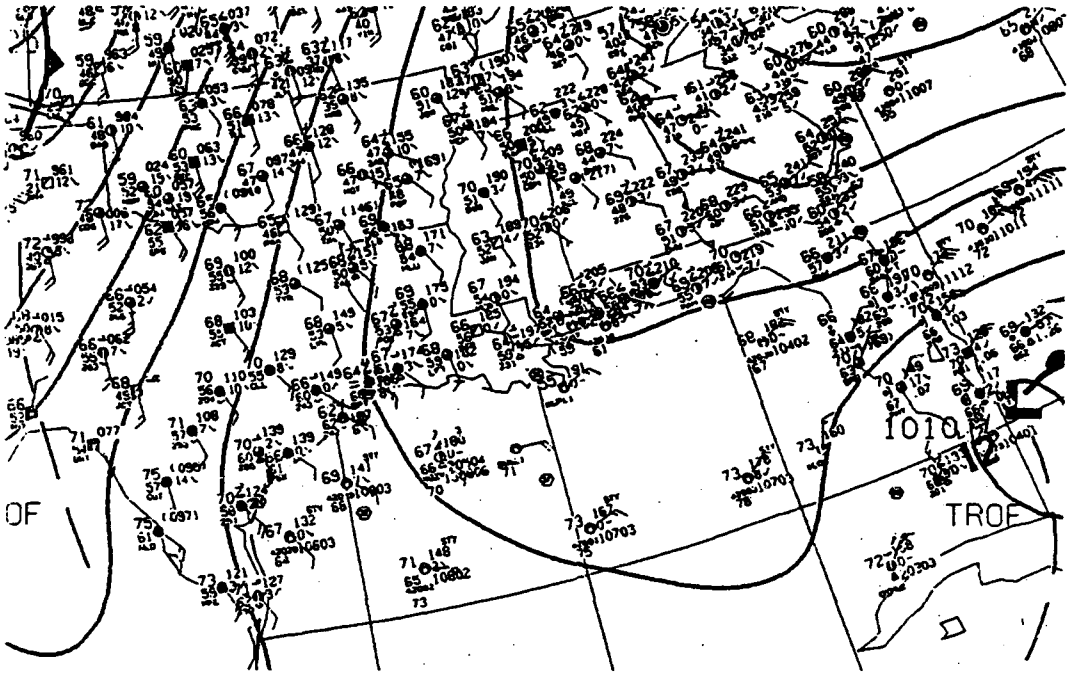

Fig. 34. As in Fig. 27, but for 00 UTC, 19 February 1994.

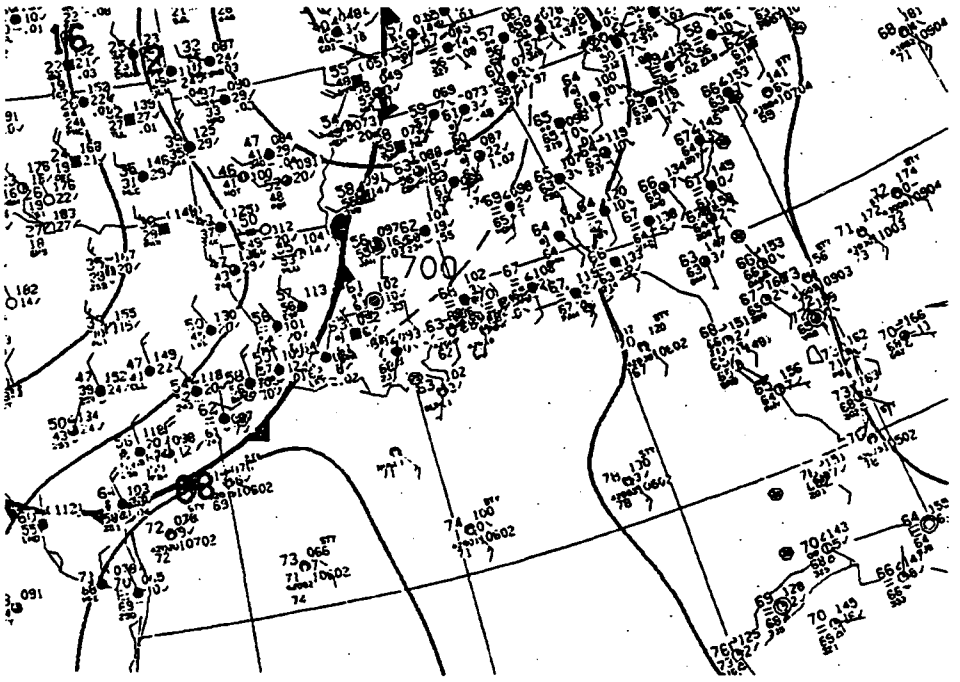

Fig. 35. As in Fig. 27, but for 1200 UTC, 23 February 1994.

and Louisiana coasts as the next cold front was moving through the area. However, by this time, the Florida Panhandle started to experience return flow, as the high pressure system had tracked far enough east that the winds had turned southerly in this region (Fig. 35). The approaching cold front passed through this area on the 24th, ending the return flow event along the entire Gulf Coast.

C. Model Performance

Statistics were performed on three different model forecast parameters and compared to the actual atmospheric values at the forecast locations: (1) height of subsidence inversion (stable layer) associated with the subtropical high pressure system, (2) amount of boundary layer cloudiness, and (3) height of the lifting condensation level (LCL). It was felt that these parameters would provide insight into the overall performance of the FSUAMT model, as all three are determined by the thermodynamic structure of the boundary layer. In all cases, the model forecasts are 24 hour forecasts valid when the model arrives at the forecast location.

1. Height of Subsidence Inversion

The height of the base of the subsidence inversion is an important factor for several reasons. First, it gives a general indication of the height of the PBL, although the PBL may not extend all the way to the base of the inversion

(Koracin and Berkowicz 1988). Also, the base of the inversion will generally be the top of any boundary layer clouds that may have formed; this information is important in aviation forecasting.

For each of the 13 cases, heights of the inversion base were compared to the actual inversion base heights. It should be noted that while an inversion did not always exist in either the model forecasted temperature profile, or the actual temperature profile, a stable layer (lapse rate less than 2 °C/km) did exist in conjunction with a very dry layer. In those cases, the base of the stable layer was used.

A scatter plot was done in order to see if there was any correlation between the forecasted heights of the inversion base and the actual inversion base heights (Fig. 36). The results are somewhat encouraging as there does

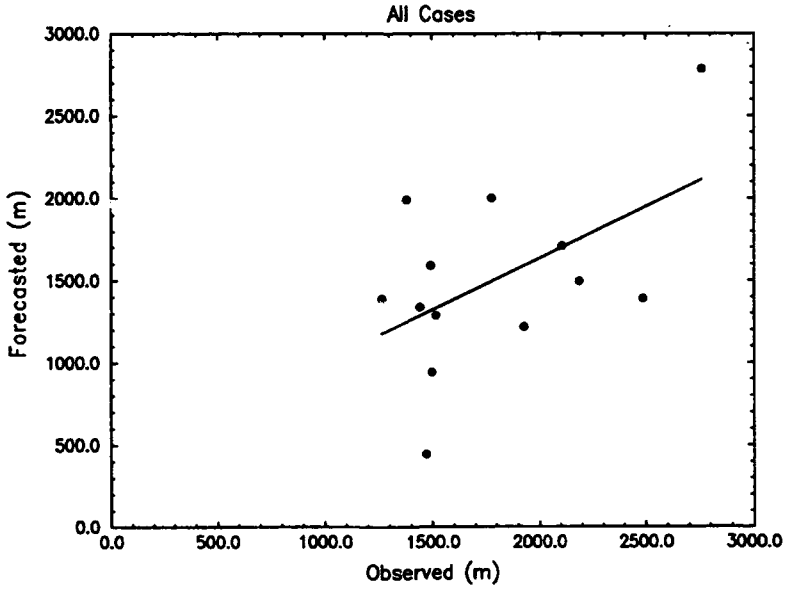

Fig. 36. Scatter plot for forecasts of inversion base height vs. observed inversion base height. Solid line indicates linear regression fit to the data. All 13 cases included.

appear to be some correlation between the observed inversion base height and the forecasted inversion base height; a correlation coefficient of 0.52 was calculated for this data set. Although this does indicate that there is some correlation between the forecasted and observed inversion base height, it is difficult to make any strong conclusions based on the small sample size in this study.

Further analysis of the scatter plot reveals that 38% of the forecasted inversion base heights were within 10% of the actual inversion base heights and that 54% were within 20% of the actual inversion base heights. Also, the FSUAMT model had a -284 m bias in forecasting the inversion base height (Table 5).

In an effort to determine under what circumstances the FSUAMT model performed well, and under what circumstances the model performed poorly, the forecasts of the inversion base height were binned into two categories - (1) two or fewer days of return flow having occurred at the forecast location, and (2) greater than two days of return flow having occurred at the forecast location. Again, even though the sample size is small, some insight into the usefulness of the model may be derived (Fig. 37).

The results of the above binning procedure are indeed somewhat informative (Table 5). The model runs in category 1 underestimated the inversion base height by only 9% (calculated by $\frac{\overline{\text{forecasted}} - \overline{\text{observed}}}{\overline{\text{observed}}}$, where the overbars indicate the mean for that variable), while for the cases in category 2, the model underestimated the height of the inversion by 26%.

The reason behind this may be threefold. The first reason may have to

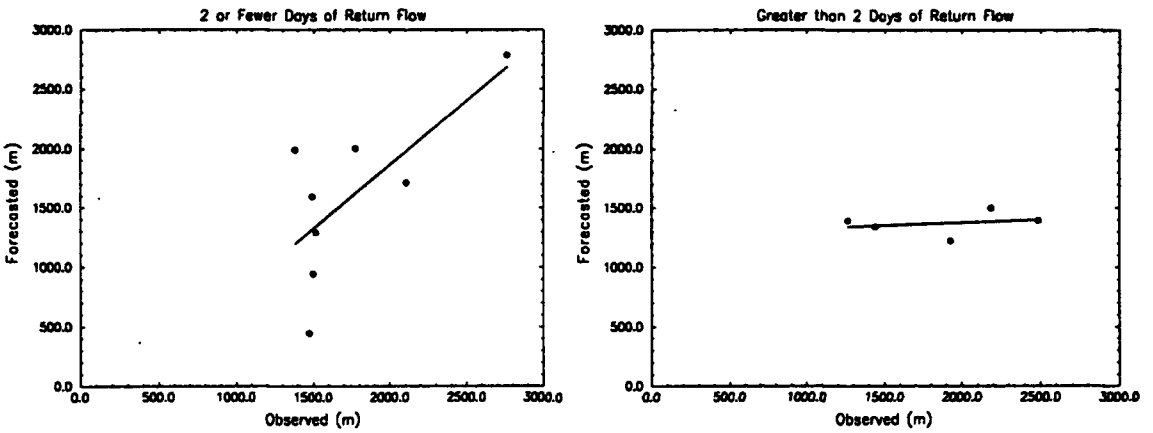

Fig. 37. As in Fig. 36, but for cases of two or fewer days of antecedent return flow (left), and for cases of greater than two days of antecedent return flow.

Table 5. Statistics comparing forecast vs. observed inversion base heights. Calculated are forecast bias, percent error in forecast (defined in text) and correlation coefficient (r). Statistics are for all cases, cases where return flow was occurring for two or fewer days, and cases where return flow had been occurring for greater than two days.

	Mean Actual Inversion Base Height (m)	Mean Fcst Inversion Base Height (m)	Bias (m)	Percent Error	r
all	1793	1509	-284	-16%	0.52
≤2 days of return flow	1751	1596	-155	-9%	0.71
> 2 days of return flow	1862	1370	-498	-26%	0.22

do with the input soundings. Although all of these cases were initialized with 00 UTC data, and thus did not exhibit radiation inversions as was discussed in chapter 2, the input soundings still tended to be unrealistically dry and cool since they are initialized using soundings over land, while the input sounding is over the Gulf of Mexico. This is not an overly serious problem when the return flow is just beginning at a particular location since the 24 hour low level trajectory does not usually start deep in the Gulf of Mexico, but rather it begins closer to shore since the winds have a more easterly and in some cases northerly component (BRO). Even though some modification will have taken place (Henry and Thompson 1976), the air is still somewhat dry and cool over the Gulf of Mexico. Thus the thermodynamic profiles over land will look somewhat similar to the profiles over water, making the input sounding somewhat realistic.

However, several days into the return flow event, the air over the Gulf will have warmed and moistened, significantly increasing the boundary layer height. However, the input sounding will not necessarily show these effects, *especially* if there are no soundings available from the southern Gulf of Mexico such as Merida, Mexico (MID); Veracruz, Mexico (VER); Belize, British Honduras (MZBZ); and Roberts Field, Grand Cayman (MKCR) (Fig. 18). The thermodynamic profiles from these southern Gulf of Mexico stations would exhibit the warming and associated PBL growth that would have occurred as the air mass moved over the Gulf (Henry and Thompson 1976). Without these soundings, the input sounding is dependent mainly on the United States soundings which will not be as warm or have a well-mixed layer as deep as a sounding over the Gulf would at this time.

Table 6. As in table 5, but for model runs with no vertical motion

	Mean Actual Inversion Base Height (m)	Mean Fcst Inversion Base Height (m)	Bias (m)	Percent Error	r
all	1793	1898	105	6%	0.49
≤2 days of return flow	1751	2076	325	19%	0.71
> 2 days of return flow	1862	1614	-238	-13%	0.98

The second reason may relate to the calculation of the prescribed vertical velocity. As the high pressure system moves east, the associated subsidence should decrease over the area. The input vertical velocities may be too strong, unrealistically suppressing the growth of the PBL. To test this hypothesis, model runs were performed for the same cases, but this time with no vertical velocity included (Table 6), and scatter plots were made (Figs. 38 and 39).

The results are interesting. Looking at all cases, the correlation coefficient drops slightly, and the bias increases to +100 m, which is not surprising since there was no subsidence to suppress the growth of the PBL. For the cases in category 1, the bias has increased to + 325 m, with the correlation coefficient remaining the same (0.71). Again, this is not surprising that there be a positive bias since it was felt that somewhat strong subsidence did exist during these particular cases, and removing that subsidence would indeed cause excessive growth of the PBL. For the cases where there were

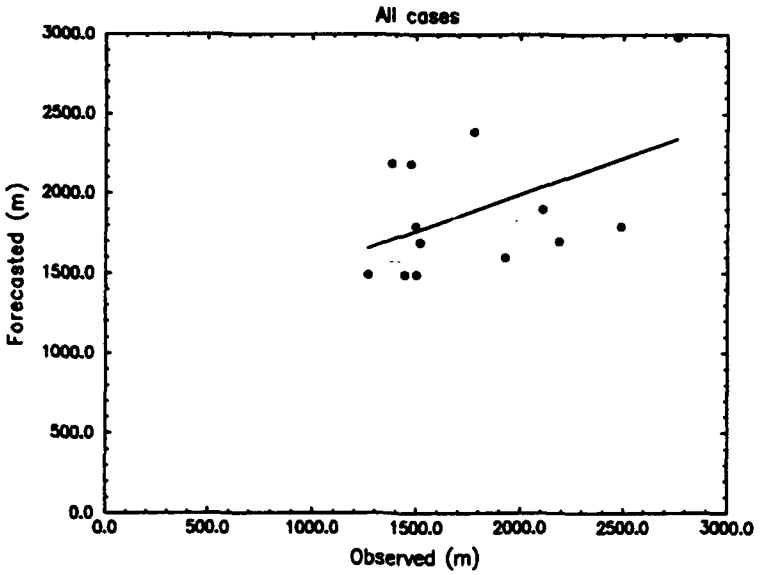

Fig. 38. As in Fig. 36, but for model runs with no vertical motion.

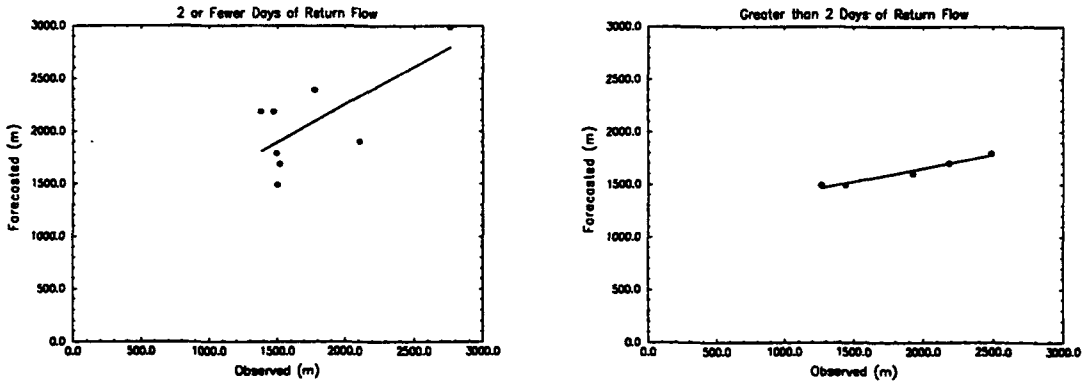

Fig. 39. As in Fig. 37, but for model runs with no vertical motion.

more than two days of antecedent return flow, the correlation coefficient increased to 0.98, and the bias also improved, to only -238 m, again related to the lack of subsidence.

The third reason that may explain the model forecasting the height of the inversion too low lies in the boundary layer winds. The PBL winds in the model are nudged to the winds from the NGM forecast. If the forecasted wind speed from the NGM is too low, then not as much mixing will take place in the PBL, and the FSUAMT model will predict the height of the inversion base too low. This problem could occur for either category, and thus could explain part of the bias that exists in the FSUAMT forecast.

Again, even though there are very few cases to look at, it would appear that there is some evidence to support the hypothesis that there is too much subsidence input into the model during category 2 cases. The fact that the average inversion base height is still too low by over 200 m is cause for belief that there may still exist another reason for the underestimation of the inversion base height, and the previously discussed hypotheses regarding the input sounding and the boundary layer winds may still be valid.

2. Amount of Boundary Layer Clouds

Another useful parameter that is important to forecasters is the amount of boundary layer clouds (N_L). A comparison was made between the forecasted amount of boundary layer clouds and the actual amount of boundary layer clouds that occurred at the arrival time of the FSUAMT model at each forecast

location (Table 7). It is important to make a note about the manner in which the FSUAMT model diagnoses N_L (Ek and Mahrt 1991). The cloud diagnosis scheme is the same one that is in the current OSU model. In that model, relative humidities must exceed 100% in order for the model to diagnose more than 50% fractional cloud coverage, as the specific humidity is actually a total water specific humidity, i.e. liquid water content is included. However, latent heat release which occurs during the formation of clouds is not taken into account. Thus for this study it was decided to take into account the latent heat release and "settle" for a maximum fractional cloud coverage of 50%.

Regardless, the model still performed very well. The different categories in table 7 indicate the amount of boundary layer clouds in octas. The category $N_L < 1$ octa is representative of clear skies (or conditions where an observation may contain a comment such as FEW CU SE, translated as: few cumulus clouds to the southeast), $1 \leq N_L < 4$ octas is representative of scattered skies, while $N_L \geq 4$ octas is representative of broken to overcast skies. The results indicate that the change to the cloud diagnosis scheme did not affect the results as both times

Table 7. Contingency table for the amount of boundary layer cloudiness predicted by the FSUAMT model vs. the actual amount of boundary layer cloudiness.

	Observed		
Forecasted	$N_L < 1$	$1 \leq N_L < 4$	$N_L \geq 4$
$N_L < 1$	3	1	0
$1 \leq N_L < 4$	0	4	2
$N_L \geq 4$	0	0	2

the model predicted a broken sky condition (maximum coverage possible), the actual conditions were broken or overcast. The difference between broken and overcast is unimportant to forecasters, as both categories indicate a ceiling, which is the concern for forecasters. Only twice did the model not predict a ceiling when one occurred.

These results bode well for the future use of the FSUAMT model in helping to forecast boundary layer cloudiness. Many flying operations are dependent on whether or not a ceiling exists. Of course, the height of the cloud base is just as critical of a forecast parameter, and is addressed in the next section.

3. Lifting Condensation Level

The height of the LCL is generally a good indication of the base height of any clouds that may form in the PBL. As such, the height of the LCL is important to forecasters, and especially to aviation forecasters. The results of the 13 cases were analyzed in a manner similar to the inversion base height. All the cases were grouped together initially, and subsequently binned into the same two categories - (1) two or fewer days of antecedent return flow, and (2) greater than two days of antecedent return flow having occurred at the forecast location. Scatter plots were made (Figs. 40 and 41), and statistics were computed for all three categories (Table 8).

The results are again encouraging. Considering all cases, the FSUAMT model overpredicted, on average, the height of the LCL by 15%, with a

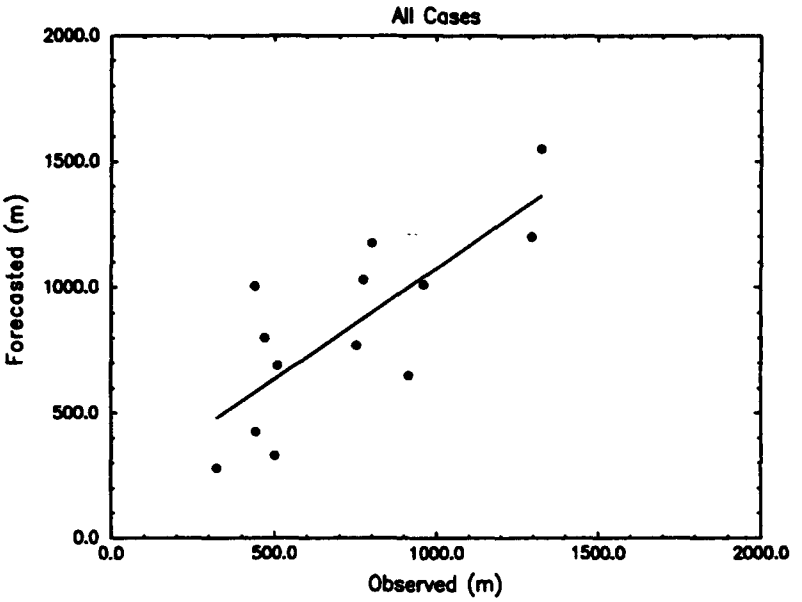

Fig. 40. Scatter plot for forecasts of height of lifting condensation level vs. observed height of lifting condensation level. Solid line indicates linear regression fit to data. All 13 cases included.

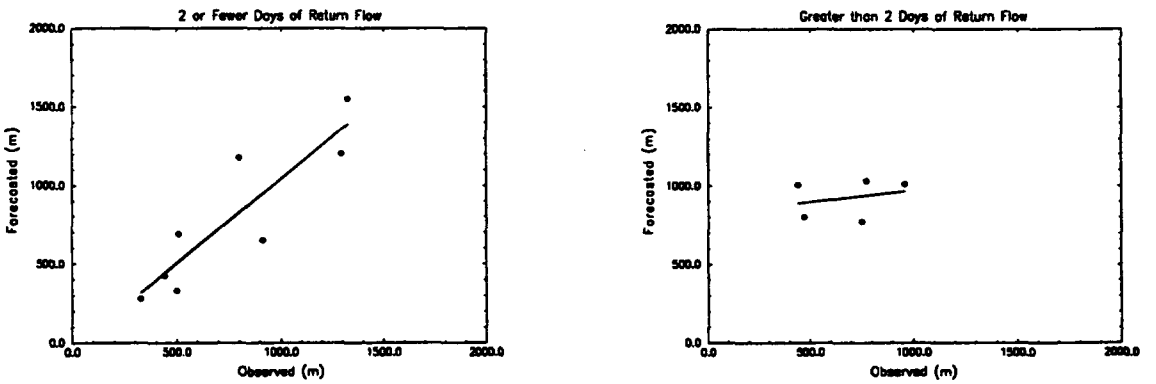

Fig. 41. As in Fig. 40, but for cases of two or fewer days of antecedent return flow (left), and for cases of greater than two days of antecedent return flow (right).

Table 8. Statistics comparing forecast vs. observed heights of the lifting condensation level (LCL). Calculated are forecast bias, percent error in forecast (defined earlier in text) and the correlation coefficient (r). Statistics are for all cases, cases where return flow was occurring for two or fewer days, and cases where return flow had been occurring for greater than two days.

	Mean Actual Height of LCL (m)	Mean Fcst Height of LCL (m)	Bias (m)	Percent Error	r
all	732	840	108	15%	0.77
≤2 days of return flow	764	788	24	3%	0.89
> 2 days of return flow	680	923	243	36%	0.26

correlation coefficient of 0.77. The average height of the LCL was 732 m, while the average of the model forecasts was 840 m, a bias of +108 m.

Comparing the two other categories, the actual height of the LCL is higher for category 1 than for category 2. This makes sense as one would expect the LCL to gradually lower during a return flow event as the air becomes increasingly moist as it stays over the Gulf of Mexico. As with the inversion base height, the FSUAMT model better predicts cases in category 1 than in category 2. For category 1, the model has a bias of only 24 m, and overpredicts the height of the LCL by only 3%, with a correlation coefficient of 0.89. The results for category 2 are very similar to the inversion base height results for the same category; the bias is large, +243 m, and the model overpredicts the height of the LCL by an average of 36%. The model is poorly correlated as well during these cases, as seen by the low correlation coefficient of 0.26.

Table 9. As in table 8, but for model runs with no vertical motion

	Mean Actual Height of LCL (m)	Mean Fcst Height of LCL (m)	Bias (m)	Percent Error	r
all	732	751	20	3%	0.58
≤2 days of return flow	764	643	-131	-17%	0.79
> 2 days of return flow	680	926	246	36%	0.09

In an effort to determine if the prescribed subsidence was again a factor in the poor performance of the model for category 2 cases, the results from the model runs with no vertical motion were looked at (Table 9). Considering all cases, the average forecast height of the LCL decreased from 840 m to 751 m, which is to be expected when the drying and warming associated with subsidence is not present. However, the correlation coefficient decreased to 0.58. The results also worsen when considering category 1 cases. Again, the average forecast height of the LCL decreased, from 788 m to 643 m, and the correlation coefficient decreased slightly from 0.89 to 0.79.

Category 2 cases exhibited a negligible change in the forecasted height of the LCL - 923 m to 926 m, but the correlation coefficient decreased to a value of 0.09, indicative of almost no correlation between the forecasted and observed LCL heights. Thus, it would appear that the hypothesis regarding subsidence being the cause of the high LCLs due to warming and drying of the PBL may not be valid, or at least another factor may be important.

This other factor may lie in the input soundings again. If the input sounding is too dry, as was always the case for category 2 days, then the model will predict a higher LCL than actually exists. This certainly seems to be the case as changing the subsidence did not affect the average forecasted height of the LCL for category 2 cases. As was mentioned earlier, it is felt that the input soundings for category 1 cases are more valid than they are for category 2 cases, and the forecasted LCL heights for category 1 cases are in much better agreement than those of category 2. It would appear then that the problem may be too much subsidence exists in the model for category 2 cases, but more importantly, the input soundings are unrealistically dry for category 2 cases, resulting in the forecasted LCL height being greater than the actual LCL height.

D. Case Studies

Three case studies will be presented to subjectively interpret the FSUAMT model's performance. In case 1, the model performed fairly well, closely predicting the thermodynamic structure of the PBL. Case 2 involves easterly flow off the Atlantic arriving at TLH. In case 3, the model did not perform as well, seriously underestimating the amount of moisture in the PBL.

1. 22 February 1994, Tallahassee, FL

The model performed fairly well in predicting the structure of the PBL at TLH at 00 UTC, 23 February 1994. The 24 hour low level trajectory started over

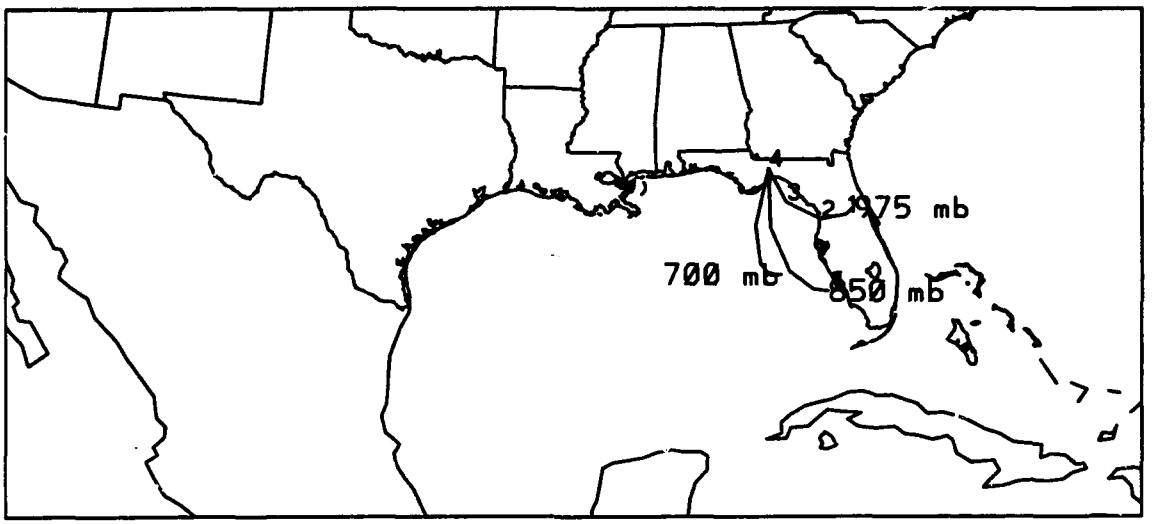

Fig. 42. As in Fig. 19, but for trajectories arriving at TLH at 00 UTC, 23 February 1994.

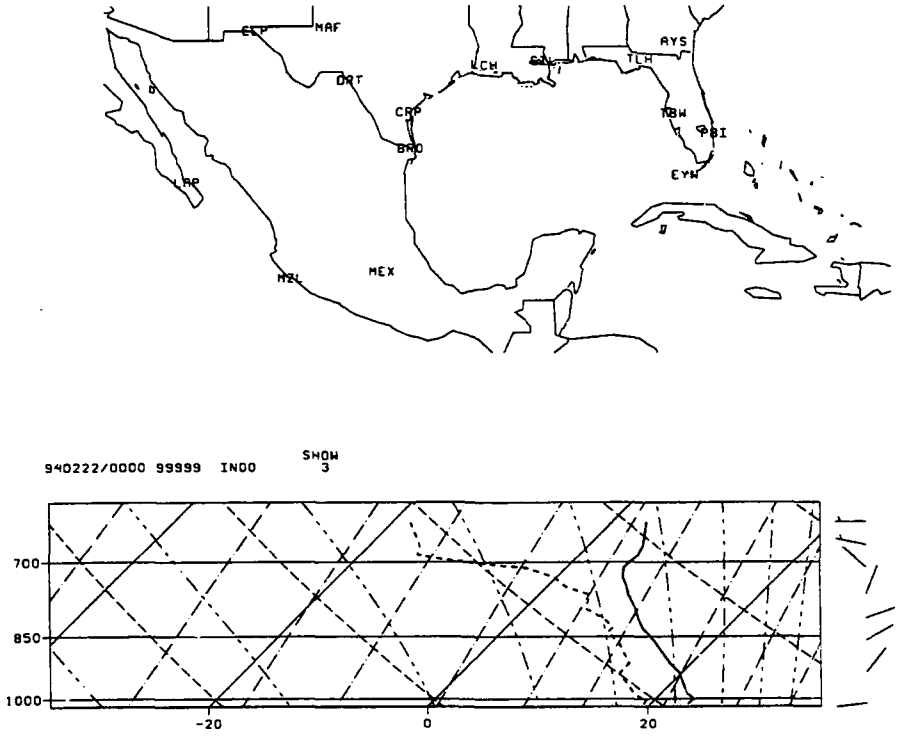

Fig. 43. Available soundings at 00 UTC, 22 February 1994 (top), and resulting composite sounding (bottom)

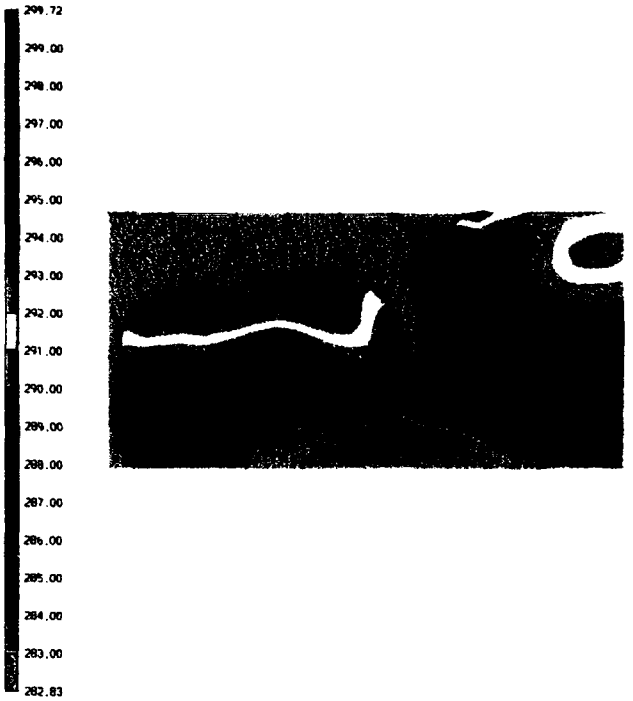

Fig. 44. Average sea surface temperatures for the week of 20 February 1994 - 26 February 1994. Temperatures (K) are given on labelbar.

the Florida peninsula (Fig. 42), which may explain why the model performed well; with the trajectories in the PBL starting over land, the input sounding was rather realistic (Fig. 43).

This case is interesting since the model starts over land, moves over somewhat cool water (17 °C) 12 hours into the model run (Fig. 44), and then moves back over land for the final 2 hours before arriving at TLH.

Comparing the forecast sounding with the observed sounding, it is seen that the model predicts the overall temperature and moisture structure of the

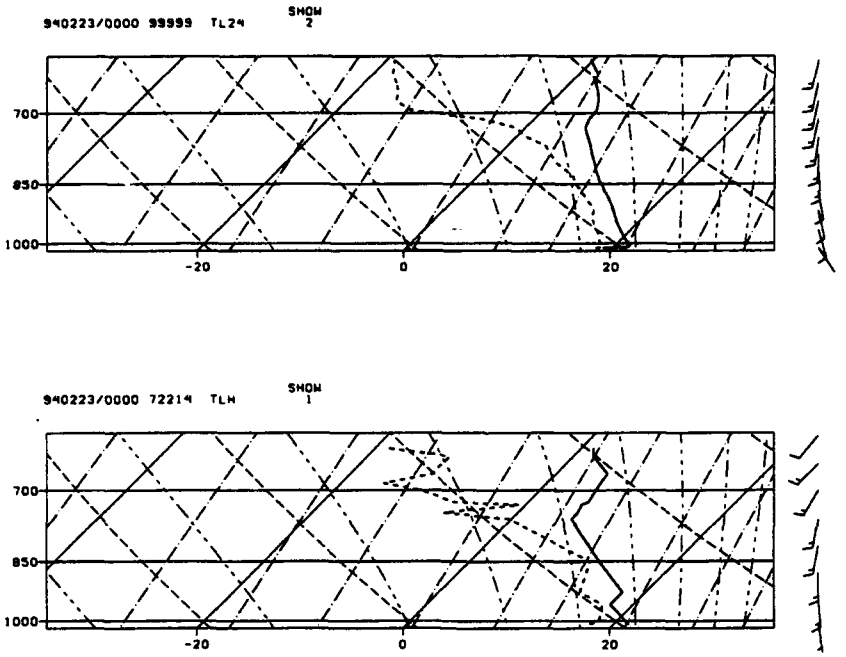

Fig. 45. The 00 UTC, 23 February 1994 forecast sounding from the FSUAMT model for TLH (top), and the observed 00 UTC sounding for TLH (bottom).

PBL very well, except near the surface where the model predicts a radiation inversion, and around 925 hPa where a slight subsidence inversion exists in the observed sounding (Fig. 45) Both the model sounding and the observed sounding contain a subsidence inversion around 700 hPa.

With regards to the overall structure of the PBL, the overall lapse rate in the forecast sounding is very similar to the actual lapse rate, with the average forecasted lapse rate (5.8 °C km^{-1}) being slightly less than the average actual lapse rate (5.9 °C km^{-1}). The forecasted moisture profile is also very similar to the actual moisture profile. The cloud base in both the forecasted and actual soundings is around 450 m, but the model only predicted scattered clouds (N_L= .13), while in reality, broken clouds existed ($N_L \geq$ .5). The model also does a good job in predicting the boundary layer winds, with both the model and actual

boundary layers containing winds from the south at 10-15 m s^{-1}.

The most glaring problem with the forecasted sounding is the shallow (60m) radiation inversion at the surface. As was discussed in chapter 2, the model's start time is one hour before the official time to take into account the fact that radiosondes are launched an hour earlier than the official time of the observation. Thus, the FSUAMT model arrives at TLH at 2300 UTC. At TLH on 22 February, the sun sets at 2327 UTC, less than 30 minutes after the arrival of the model. However, radiation sunset (when the surface effectively receives no incoming solar radiation) occurs earlier than the actual sunset; therefore, the model starts to cool the surface by 2300 UTC. Since the model only predicts scattered boundary layer clouds, it allows the surface to radiate its energy to space and via a negative turbulent heat flux, cools the model levels up to 60 m, forming a radiation inversion. Since in reality the amount of boundary layer clouds was substantial, most of the longwave radiation emitted by the surface was blocked by the clouds, not allowing the lowest levels to cool as rapidly; thus a radiation inversion did not form.

2. 18 February 1994, Tallahassee, FL

As was mentioned earlier in this section, 24 hour back trajectories from the Atlantic Ocean arrived at TLH at 00 UTC, 19 February 1994 (Fig. 46). It was felt that this would be a good case to test if the model could accurately forecast easterly flow off the Atlantic that moved over the warm waters of the Gulf Stream. The model was initialized over the relatively cool water (17.9 °C) south

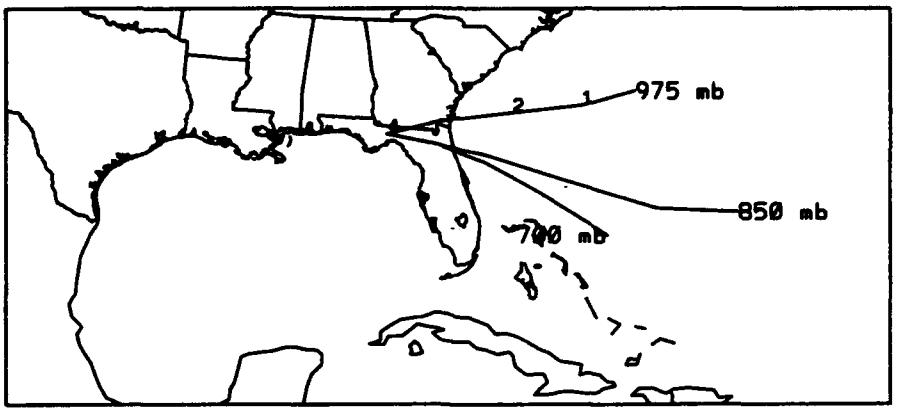

Fig. 46. As in Fig. 19, but for trajectories arriving at TLH at 00 UTC, 19 February 1994.

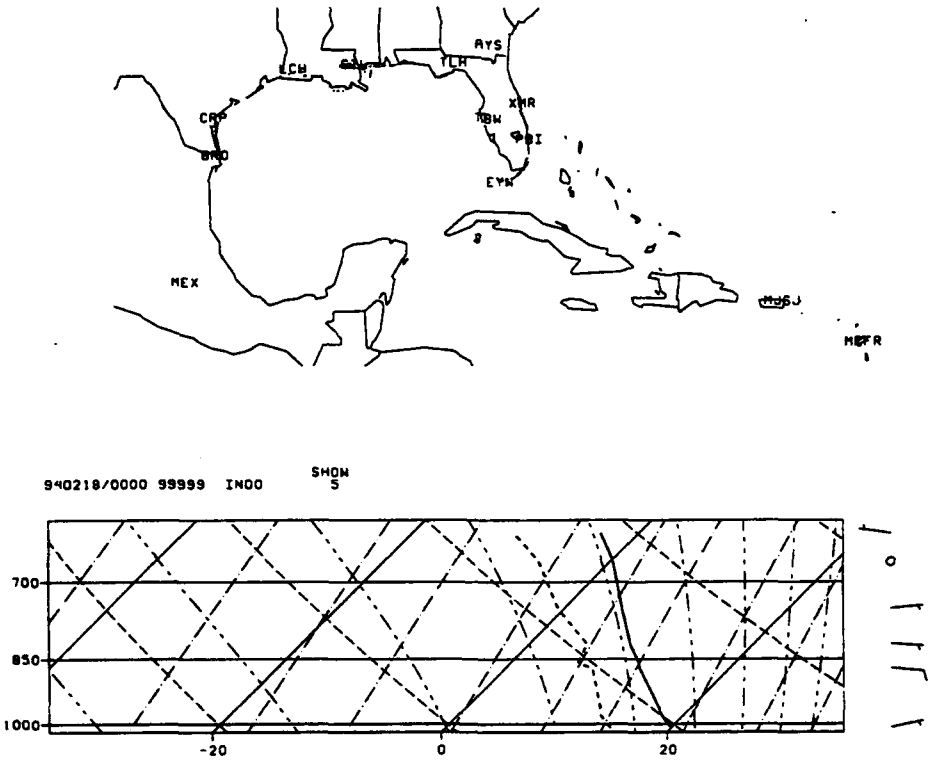

Fig. 47. As in Fig. 43, but for 00 UTC, 18 February 1994.

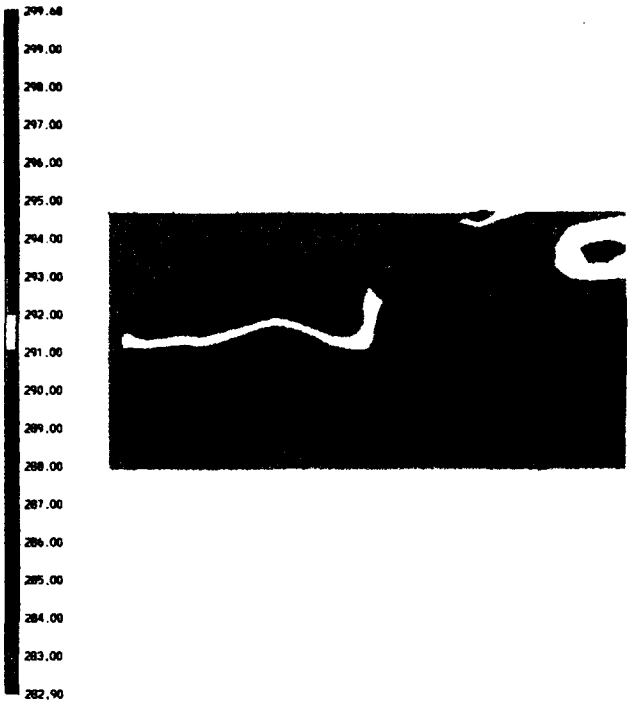

Fig. 48. As in Fig. 44, but for the week of 13 February 1994 - 19 February 1994.

of the Gulf Stream (Figs. 47 and 48), and then moved eastward over the Gulf Stream, and then onto land for the last 6 hours of the model run.

In an effort to visualize the thermodynamic changes to the PBL as the model moved over these different environments, time sections of the potential temperature and mixing ratio were made (Fig. 49). The boundary layer initially cools and moistens since the input sounding is both too warm and too dry for air over the cool gyre of water south of the Gulf Stream. As the model moves over the Gulf Stream, some warming does take place, but not much. However, the

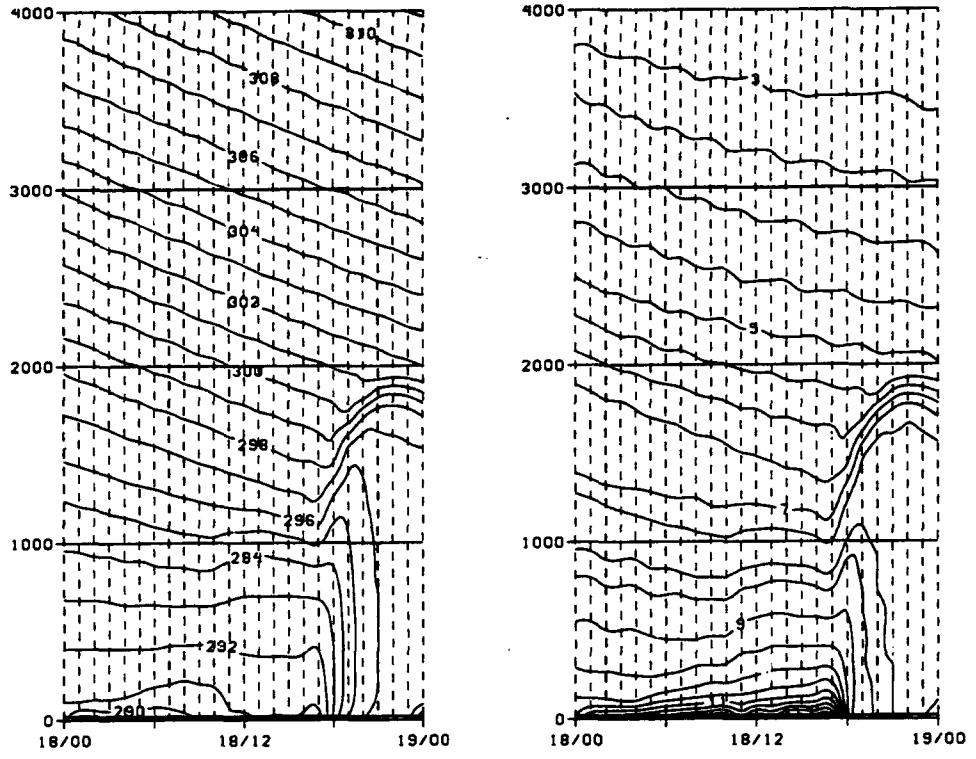

Fig. 49. Twenty-four hour time sections of potential temperature (K) (left) and mixing ratio (g kg^{-1}) (right). Dashed lines represent one hour.

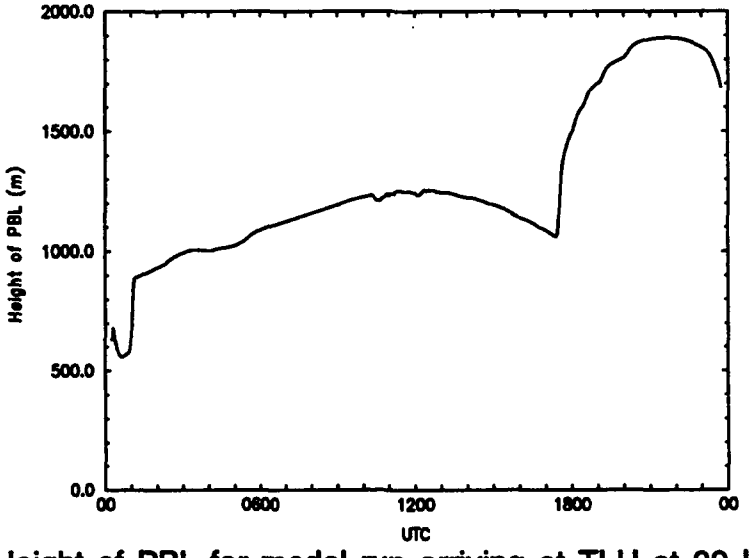

Fig. 50. Height of PBL for model run arriving at TLH at 00 UTC, 19 February 1994.

boundary layer does increase (Fig. 50); so it would appear that the sensible heating that is occurring is going into increasing the boundary layer depth, and not into warming the PBL. Some tightening of the isentropes and isohumes is evident around this time, indicating a strengthening of the inversion at the top of the PBL.

Notice that once the model moves onshore, the boundary layer rapidly warms and dries out, and increases its depth by 800 m. The capping inversion strengthens as both the isentropes and isohumes are even more tightly packed. By 2200 UTC, a well-mixed layer has formed, and by 00 UTC, a surface inversion can be seen in the time section as the lowest portion of the PBL begins to cool.

The final sounding was again compared to the observed sounding (Fig. 51). The model is too warm throughout the boundary layer by an average of approximately 3 °C. Thus, even though the model correctly predicted the PBL moisture field, the lower relative humidity throughout the PBL resulted in a lack of cloudiness. This is again probably the reason for the surface-based inversion in the model. Although the observed sounding does appear moist enough to support a substantial amount of boundary layer cloudiness, only 1 octa of clouds was reported at this time. In fact a more stable layer can be seen at the surface of the actual sounding, indicative of an inversion starting to form, which is present in the 1200 UTC sounding on the 20th. In this case, the model underestimates the PBL winds by around 5 m s^{-1}, which may be the reason that the actual subsidence inversion is located higher than the forecasted inversion.

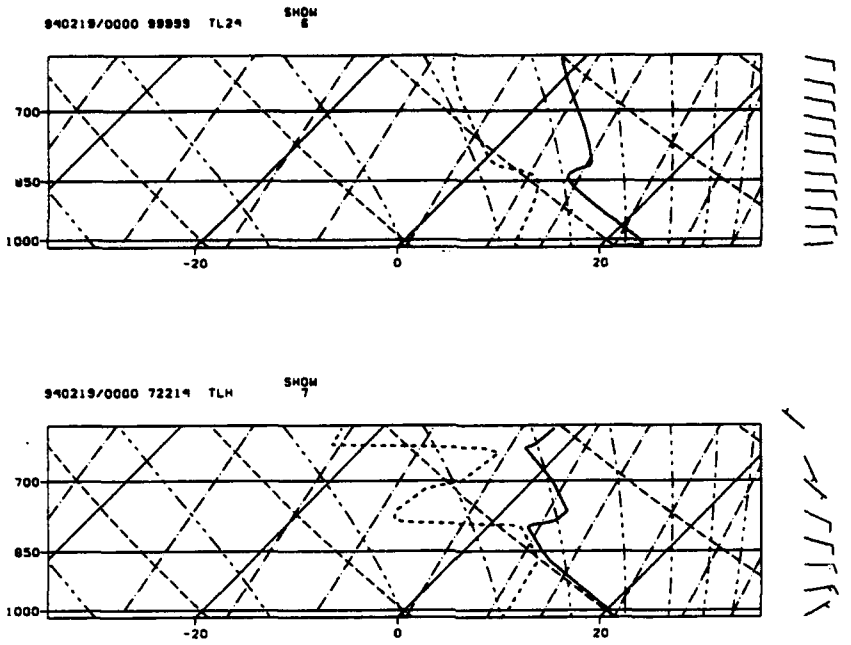

Fig. 51. As in Fig. 45, but for 00 UTC, 19 February 1994.

3. 19 February 1994, Brownsville, TX

By 19 February, BRO was experiencing its third day of return flow. The low-level trajectory which arrived at BRO at 00 UTC on the 20th, started over the warm water (22.1 °C) in the Bay of Campeche, and then moved north over increasingly cooler waters (Figs. 44 and 52). The input sounding contains a fairly realistic temperature profile; however, the moisture profile is unrealistically dry considering all trajectories up to 850 hPa start over the Bay of Campeche (Fig. 53). The input sounding is heavily influenced by the sounding from Mexico City, Mexico (MEX) which is very dry due to the fact that its elevation is 2234 m. The absence of a sounding at MID also causes the input sounding to be too dry.

When the model arrives at BRO at 00 UTC on the 20th, it has formed a

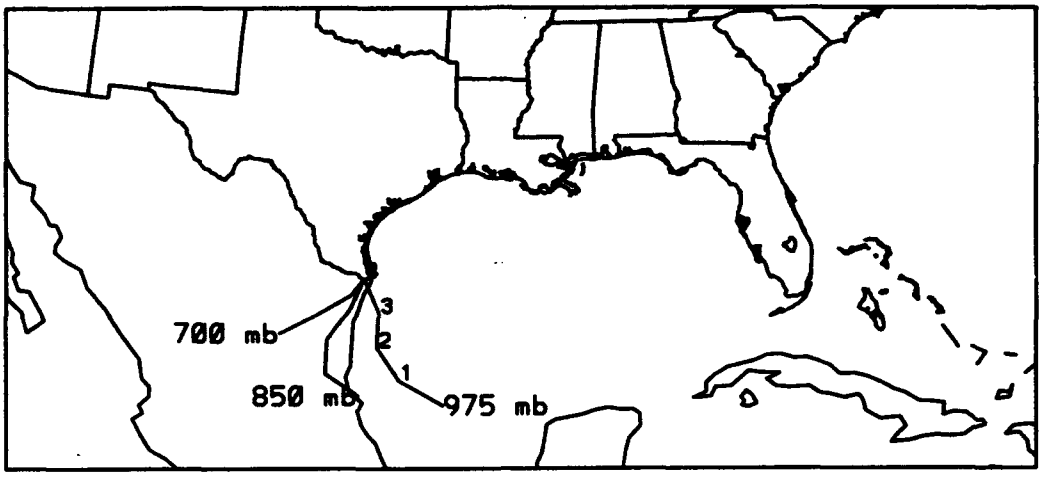

Fig. 52. As in Fig. 19, but for trajectories arriving at BRO on 00 UTC, 20 February 1994.

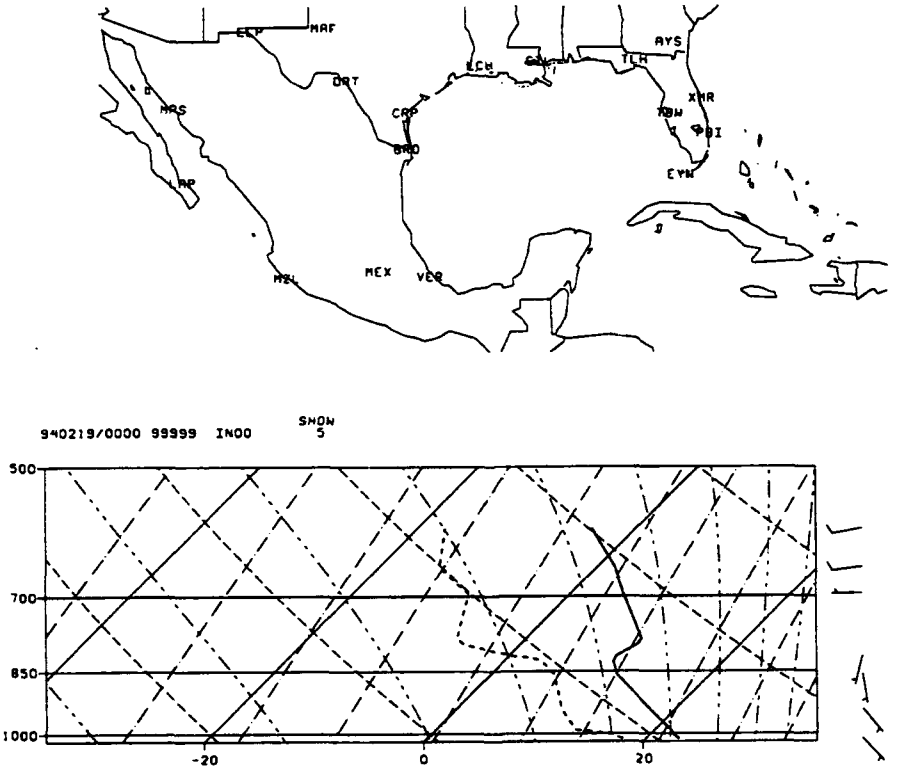

Fig. 53. As in Fig. 43, but for 00 UTC, 19 February 1994.

well-mixed layer in both temperature and moisture up to the subsidence inversion (Fig. 54). The model underpredicts the height of the subsidence inversion base slightly (100 m), compared to the actual subsidence inversion base. The model sounding is much too dry, causing the predicted LCL height (1005 m) to be much higher than the actual level of the LCL (440 m).

In an effort to determine if the input sounding was the cause of the poor moisture forecast, an artificial input sounding was made with the same temperature profile as before, but a bogus moisture profile was added, based on the discussion in chapter 2 regarding the soundings from dropwinsondes in the Gulf of Mexico. The model did indeed predict a much more realistic moisture profile as the PBL is well-mixed in moisture up to the LCL, where it becomes saturated until the subsidence inversion is reached (Fig 55). The corresponding

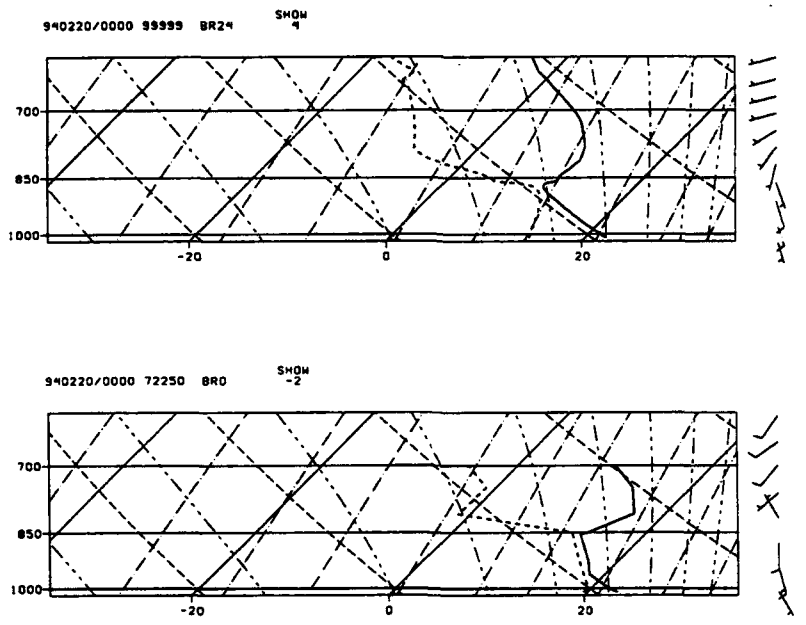

Fig. 54. As in Fig. 45, but for BRO at 00 UTC, 20 February 1994.

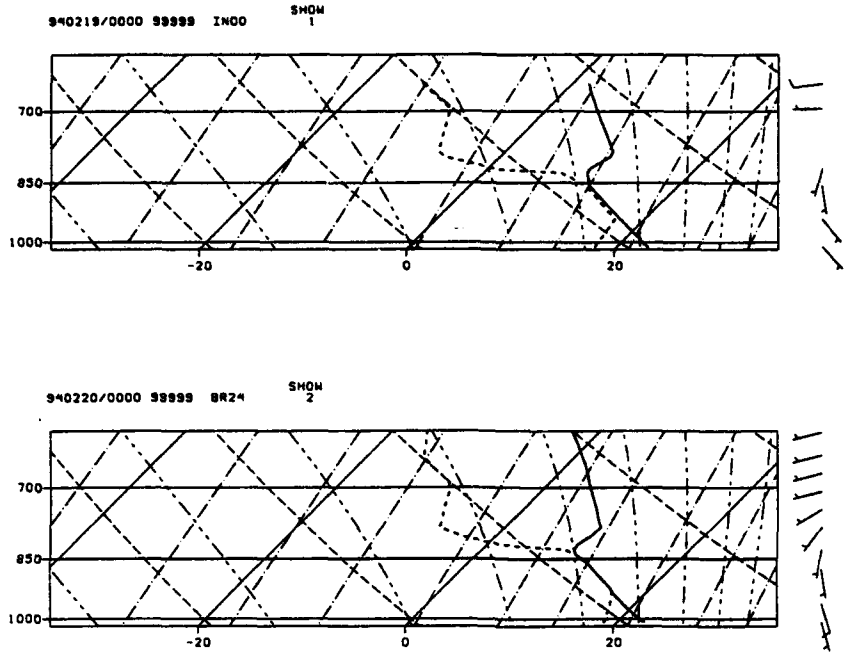

Fig. 55. Bogus initial sounding at 00 UTC, 19 February 1994 (top), and resulting forecast sounding for BRO at 00 UTC, 20 February 1994 (bottom).

LCL is much more realistic as well (520 m).

Time sections of mixing ratio for both model runs provide some insight into the processes that are occurring (Fig. 56). With the actual initial profile, the model moistens the entire boundary layer in response to the moisture flux from the Gulf of Mexico. Not until 12 hours into the model run does the model begin to moisten the lowest levels, but the upper boundary layer around 1000 m is still 5-20% drier than the boundary layer predicted using the bogus moisture profile. Thus, once the model moves onshore and the boundary layer expands, the air entrained into the boundary layer is much drier, and the PBL dries out very quickly. For the model run with the bogus moisture profile, the air at the top of the boundary layer is already very moist (10 g kg^{-1}); so when the boundary layer

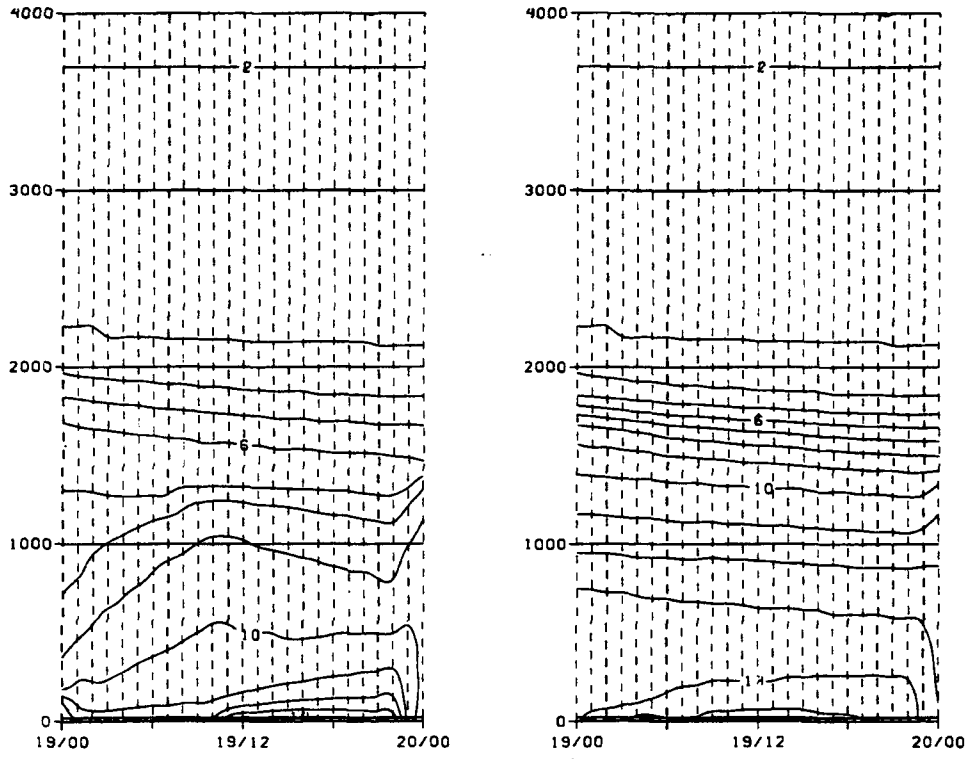

FIG. 56. Time sections of mixing ratio (g kg^{-1}) for model runs arriving at BRO at 00 UTC, 20 February 1994. Left panel contains time section for the actual input sounding; right panel contains time section for initial sounding with bogus moisture.

expands, the dry air entrained from aloft does not mix as effectively down to the lower levels of the PBL as it does with the drier initial profile.

E. Conclusions

The newly developed FSUAMT model does show some promise in its ability to forecast return flow events, especially at the onset of return flow events. Although the sample size is small, it does appear that the model is able to forecast the height of the subsidence inversion base and the LCL, as well as the

amount of boundary layer cloudiness - all important forecasting parameters.

The FSUAMT model's forecasts of the inversion base height had a correlation coefficient of 0.52 compared to the actual inversion base heights, when all cases were considered. After binning the cases into two categories - (1) two or fewer days of return flow occurring at a location, and (2) greater than two days of return flow occurring at a station, it was seen that category 1 days were better correlated (0.71) than were category 2 days (0.22) with the observed inversion base heights. Looking at the same cases without subsidence lowered the overall correlation to 0.49, but increased the correlation for category 2 days (0.98) and resulted in a better bias as well. Whereas for category 1 days, the bias increased from -155 m to + 325 m. This lends credence to the idea that the prescribed subsidence for category 2 days may be too strong, artificially suppressing the PBL.

A similar dichotomy between categories existed as well in the calculation of the LCL height. Overall, the model had a correlation coefficient of 0.77 when compared to the observed LCL height, but the category 1 days were better correlated than the category 2 days, 0.89 to 0.26. Removing the subsidence lowered the correlation coefficients for both categories. This result led to the belief that since the input soundings are unrealistically dry, as was discussed in chapter 2, the model forecast of the boundary layer would be too dry, causing the LCL to be too high as well. This hypothesis was tested for a case involving trajectories arriving at BRO at 00 UTC, 20 February 1994. A realistic moisture profile was bogused into the initial sounding, and the result was a much more realistic forecast of the moisture in the PBL and the resultant LCL height.

The model forecasted the amount of boundary layer cloudiness very well. For both cases that the model predicted greater than 4 octas of cloud coverage, the observed cloud coverage was also greater than 4 octas. Similarly, the model predicted less than 1 octa of cloud coverage in 4 cases: in 3 of those cases, less than 1 octa was observed, and in the other case, less than 4 octas were observed.

It would appear then that the critical factors that still need to be resolved are the input soundings and the prescribed vertical motion field, especially in cases where the return flow has been occurring for more than two days. These two factors, and what can be done about them, will be discussed in the next chapter.

CHAPTER 5. CONCLUSIONS AND FUTURE WORK

The first part of this chapter will discuss conclusions from the minimum temperature study and from the FSUAMT model runs. Then a look at future work, which has been alluded to throughout this paper, will be presented, along with suggestions.

A. Conclusions

1. Minimum Temperature Study

Often in winter, after passage of a cold front, TLH has the coldest minimum temperature of any station in the Southeast. Although it has never been proved, the primary reason given for this discrepancy is cold-air drainage. However, it was felt that the cold temperatures could be explained simply by radiative effects. To test this hypothesis, a locally modified version of the OSU 1-d PBL model, now containing the more consistent Geleyn (1988) formulation for the diagnosis of the 2 m air temperature, was used. It was felt that if the model, with its surface energy balance and crude radiative parametrization, could accurately forecast the cold temperatures, then the radiation hypothesis would be strengthened.

In conjunction with a study done by Fuelberg and Elsner (personal communication, 1994), 16 days from 1993 were selected as cases to use the

model on. The criteria used to select the days were winds less than 5 kt and no ceiling for at least 6 hours before the minimum temperature. It was felt that the PBL model would perform best under these conditions.

Twelve and 24-hour forecasts from the PBL model were compared to 12 and 24-hour forecasts from the LFM, NGM, persistence and climatology. Considering all 16 days, the PBL model forecasts of the minimum temperature had correlation coefficients of 0.74 (24 hour forecast) and 0.87 (12 hour forecasts) when compared to the actual minimum temperatures. Both 12 and 24- hour forecasts from the NGM and LFM had correlation coefficients of approximately 0.95.

However, the PBL model was much less biased than either of the large scale models, with the 12-hour forecast from the PBL model having a bias of only 0.33 °F, compared to a bias of 3 °F for the 24-hour NGM forecast and a 7.15 °F bias for the 12-hour LFM forecasts.

There were several days in the study where advection of moisture and/or temperature could account for poor forecasts made by the PBL model. If those days are disregarded, then the correlation coefficients for both the 12 and 24-hour PBL forecasts increase to over 0.9. Also, the bias improves dramatically for the 24-hour PBL forecast, from -3.42 °F to -0.6 °F. Thus the correlation coefficients for the PBL model are comparable to either of the large scale models, but the bias is lower.

With these statistics, it is clear that the cold-air drainage hypothesis used to explain the cold temperatures at TLH may not be valid, and instead the phenomenon may be due simply to radiative processes. Thus, the PBL model

would be a useful tool in forecasting daily temperature extremes during periods of light synoptic forcing at a location such as TLH.

2. Florida State University Air Mass Transformation Model

The motivation behind the development of the Florida State Un / Air Mass Transformation (FSUAMT) model was discussed in chapter 1: the NGM does not do an adequate job in forecasting return flow events, with advection being the dominant process instead of air mass modification due to the fluxes of heat and moisture from the Gulf of Mexico (Janish and Lyons 1992). Also, as was seen in the minimum temperature study, the 1-d PBL model does not perform well in cases where advection is important. Thus the high resolution 1-d PBL model was modified to move along a low-level trajectory, so that surface fluxes of heat and moisture as the air mass moved over the warm waters of the Gulf of Mexico would be incorporated. Also, by using the method of Holtslag *et al.* (1990) to determine an input sounding, differential advection could be accounted for in the model. This is important, as a frequent source of air at 700 hPa and above during return flow events is the Mexican plateau, where the air is very dry. Simply using a 1-d profile at the starting point of the low-level trajectory could not take into account this process.

Several cases from a return flow event that occurred from 17 February - 23 February 1994, and two cases from the end of a return flow event that occurred 26 January - 27 January 1994, were examined to determine the effectiveness of the newly developed (FSUAMT) model. Three model output

parameters were compared to the observed parameters: height of the subsidence inversion base, amount of boundary layer cloudiness, and height of the lifting condensation level (LCL). The three were chosen since they are all determined by the thermodynamic structure of the PBL.

The model forecasted the amount of boundary layer cloudiness very well. Only twice did the model incorrectly forecast the amount of boundary layer cloudiness when a ceiling existed. In fact, for the cases in which the model predicted a ceiling, a ceiling was observed. These results bode well for using the FSUAMT model to predict boundary layer cloudiness during return flow events.

It was shown that for the subsidence inversion base and for the height of the LCL, the FSUAMT model's forecasts were more highly correlated with the observed values and had smaller biases during cases where the return flow had been occurring for two or fewer days (category 1), than for cases where the return flow had been occurring longer (category 2).

It was hypothesized that the prescribed subsidence was too strong for the category 2 cases, and the same model runs were performed with no input vertical velocity. The results were interesting with regard to the subsidence inversion base as the correlation increased from 0.22 to 0.98 for category 2 cases, with the bias going from -498 m to -238 m. As expected, for category 1 days the bias increased from -155 m to 325 m, since it was felt that somewhat strong subsidence did exist over the area for those days.

The results were much less encouraging with regard to the height of the LCL when the subsidence was removed. In both categories, the bias increased

and correlation coefficients decreased. It was thus felt that another factor may be important in explaining the differences in correlation between the 2 categories for forecasting the LCL height. Namely, the input sounding was too dry, causing the FSUAMT model to underforecast the amount of boundary layer moisture, resulting in the forecasted height of the LCL to be too high.

To test this theory, a realistic moisture profile was bogused into an input sounding for a case where trajectories that arrived at Brownsville, TX (BRO) at 00 UTC, 20 February 1994, started over the warm waters (22 °C) of the Bay of Campeche. The results were encouraging as the model initialized with the bogus moisture profile gave a more accurate prediction of the LCL height (520 m) than when the actual input sounding was used (1005 m), with an observed LCL height of 440 m.

Two other cases that the model predicted fairly well were looked at in more detail. One case involved easterly flow off the Atlantic arriving at TLH, and the other case involved flow that originated over the Florida Peninsula arriving at TLH 24 hours later. In both cases, the model was able to accurately forecast the thermodynamic structure of the PBL as it moved over different environments.

Thus although the sample size is somewhat small, the FSUAMT model has shown an ability to accurately forecast the structure of the PBL during a return flow event. Further study still needs to be performed to fully determine the effectiveness of the model for all return flow events, but the results from this study of one particular return flow event are an encouraging sign for future use of this model to forecast PBL structure during return flow events.

B. Future Work

1. Minimum Temperature Study

In order to further solidify the hypothesis that the cold temperatures at TLH can be explained by radiative processes, and not by cold-air drainage, data from late 1991 (after the move of the rawinsonde site from Apalachicola, FL, to TLH) and 1992 will be examined to determine which days meet the criteria discussed earlier. It is hoped that the additional results from the use of the PBL model can be used in conjunction with studies currently being performed by Fuelberg and Elsner (personal communication, 1994) to further support the radiative processes hypothesis.

2. Florida State University Air Mass Transformation Model

More case studies need to be examined to definitively determine the cause of the model's poor performance during cases where return flow was occurring for greater than 2 day. This present study certainly gives indications that the initial representation of the boundary layer moisture is unrealistically dry, and that perhaps the prescribed subsidence is too strong. Possible solutions to these problems, as well as additional future work that may be done will be discussed next.

a) DETERMINATION OF INPUT SOUNDING

The first step towards improving the model would be improving the input sounding. A method of determining a more realistic input moisture profile must be developed. One solution may be to use large scale model output over the Gulf of Mexico to help get a more realistic representation of the PBL moisture. The problem with this solution is that it has been shown that the NGM also underestimates the amount of boundary layer moisture during return flow events, although the amount of underrepresentation is not as severe as it is for some of the cases in this study. Another solution may present itself in the next few months with the launching of the next Geostationary Operational Environmental Satellite (GOES). This satellite, GOES-I, will be able to provide atmospheric soundings on a regular basis. If these data become available and are shown to be reliable, they could be of great use for the determination of an input sounding, as they would provide a realistic representation of the thermodynamic structure of the PBL.

b) INPUT VERTICAL MOTION FIELD

It is unclear how to solve this problem. One solution may be to use the vertical motion fields forecasted by the large scale models. However, an attractive feature of the current procedure is that GEMPAK calculates the vertical motion field using current, observed data from radiosondes and is not forecasting the vertical motion, as the large scale models do.

Another solution would be to use no vertical motion, as is the case in Holtslag *et al.* (1990). However, it is felt that this would be unrealistic, especially at the onset of a return flow event when subsidence is likely to be significant, and lead to even more unrealistic results.

c) CLOUD DIAGNOSIS SCHEME

As was mention in chapter 4, the current cloud scheme does not allow for greater than 50% fractional cloud coverage. This is somewhat unrealistic during return flow events, although for only 4 of the cases in this study was there greater than 50% cloud coverage.

One solution would be to use the cloud diagnosis scheme from older versions of the OSU 1-d PBL model. In this scheme, the fractional amount of boundary layer cloudiness, N_L, is given by (Ek and Mahrt 1989)

$$N_L = \left(\frac{RH - RH_{crit}}{1 - RH_{crit}} \right)^2 \tag{29}$$

where for the stable PBL, RH_{crit}=0.8, and RH is the maximum relative humidity in the PBL. For the unstable PBL, the above calculation is performed, and a calculation with RH_{crit}=0.7, and RH as the relative humidity at the level of the LCL is also performed. To avoid instabilities, the maximum of these two values is used for the determination of N_L in the unstable boundary layer.

An alternative method would involve dividing the total water content into

water vapor content, and liquid water content. In this manner, latent heat release could be accounted for, and N_L could exceed 0.5. Researchers at OSU are currently working on this problem (Ek personal communication, 1994). This would be an important improvement, not only for the cloud scheme, but also because the transmissivity of longwave radiation is dependent on the liquid water content in the atmosphere.

d) TRAJECTORIES

As was mentioned in chapter 2, the trajectories used in this study are based on NGM forecasts. Since the results of the FSUAMT model are somewhat heavily dependent on the trajectory the model follows, it may behoove future researchers to acquire another source of trajectories. The benefits would be threefold. First, another trajectory source would help determine the accuracy of the NGM-based trajectories. Second, if it is known that the NGM is not forecasting a return flow event well, then without another source of trajectories, a forecaster would be forced to use the NGM-based trajectories, and thus the accuracy of the FSUAMT model forecasts would be in doubt. Third, additional arrival times of the trajectories would be beneficial. For example, an arrival time of 1800 UTC could help in the forecasting of afternoon thunderstorm activity.

e) SEA SURFACE TEMPERATURES

The current resolution of the SSTs, in both time and space, may not

sufficiently represent the gradient of temperature that exists close to shore at the continental shelf break. The water between the shore and the shelf break is often very shallow, and thus is more prone to rapid temperature changes as cold air masses move over the water than is the deeper water in the middle of the Gulf of Mexico. It is likely that operational meteorological centers, such as NMC and the Air Force Global Weather Center, do have higher resolution SST fields that may be available for future use of the FSUAMT model.

3. Conclusions

It is felt that the above suggestions will further enhance the performance of the FSUAMT model, and enable it to be used as a valuable forecasting tool at Air Force base weather stations in the future.

References

Burk, S. D., and W. T. Thompson, 1992: Airmass modification over the Gulf of Mexico: mesoscale model and airmass transformation model forecasts. *J. Appl. Meteor.*, **31**, 925-937.

Crisp, C. A., and J. M. Lewis, 1992: Return flow in the Gulf of Mexico. Part I: a classificatory approach with a global historical perspective. *J. Appl. Meteor.*, **31**, 868-881.

Deardorff, J. W., 1966: The countergradient heat flux in the lower atmosphere and in the laboratory. *J. Atmos. Sci.*, **23**, 503-506.

Ek, M., and L. Mahrt, 1989: *A User's Guide to OSU1DPBL version 1.0.3*, Department of Atmospheric Sciences, Oregon State University, Corvalis, OR. 106 pp.

Ek, M., and L. Mahrt, 1991: *OSU 1-D PBL Model User's Guide version 1.0.4*, Department of Atmospheric Sciences, Oregon State University, Corvalis, OR. 232 pp.

Geleyn, J.-F., 1988: Interpolation of wind, temperature and humidity values from model levels to the height of measurement. *Tellus*, **40A**, 347-351.

Henry, W. K., and A. H. Thompson, 1976: An example of polar air modification over the Gulf of Mexico. *Mon. Wea. Rev.*, **104**, 1324-1327.

Holtslag, A. A. M., 1987: Surface fluxes and boundary-layer scaling; models and applications. KNMI Sci Rep. 87-02.

Holtslag, A. A. M., E. I. F. DeBruin, and H.-L. Pan, 1990: A high resolution air mass transformation model for short-range weather forecasting. *Bound.-Layer Meteor.*, **118**, 1561-1575.

Janish, P. R., and S. W. Lyons, 1992: NGM performance during cold-air outbreaks and periods of return flow over the Gulf of Mexico with emphasis on moisture-field evolution. *J. Appl. Meteor.*, **31**, 995-1017.

Koracin, D., and R. Berkowicz, 1988: Nocturnal boundary-layer height: observations by acoustic sounders and predictions in terms of surface-layer parameters. *Bound.-Layer Meteor.*, **43**, 65-83.

Lewis, J. M., and C. A. Crisp, 1992: Return flow in the Gulf of Mexico. Part II: variability in return-flow thermodynamics inferred from trajectories over the Gulf. *J. Appl. Meteor.*, **31**, 882-898.

Leyton, L., E. R. C. Reynolds, and F. B. Thompson, 1967: Rainfall interception in forest and moorland in W. E. Sopper and H. W. Lull (eds.), *Forest Hydrology*, Pergamon, Oxford, pp. 163-178.

Louis, J.-F., M. Tiedtke, and J.-F. Geleyn, 1982: A short history of the operational PBL-parametrization of ECMWF. Workshop on planetary boundary-layer parametrization, European Centre for Medium Range Weather Forecasts, Shinfield Park, Reading, Berks, U.K.

Mahrt, L., and H. Pan, 1984: A two-layer model of soil hydrology. *Bound.-Layer Meteor.*, **29**, 1-20.

Mailhot, J., 1992: Numerical simulation of airmass transformation over the Gulf of Mexico. *J. Appl. Meteor.*, **31**, 946-963.

O'Brien, J. J., 1970: Alternative solutions to the classical vertical velocity problem. *J. Appl. Meteor.*, **9**, 197-203.

Pan, H.-L., and L. Mahrt, 1987: Interaction between soil hydrology and boundary-layer development. *Bound.-Layer Meteor.*, **38**, 185-202.

Reiff, J., D. Blaauboer, H. A. R. DeBruin, A. P. van Ulden, and G. Cats, 1984: An air mass transformation model for short-range weather forecasting. *Mon. Wea. Rev.*, **112**, 393-412.

Reynolds, R. W., 1988: A real-time global sea surface temperature analysis. *J. Climate*, **1**, 75-86.

Reynolds, R. W., and D. C. Marsico, 1993: An improved real-time global sea surface temperature analysis. *J. Climate*, **6**, 114-119.

Reynolds, R. W., and T. S. Smith, 1993: Improved global sea surface temperature analysis. Submitted to *J. Climate.*

Stull, R. B., 1988: *An Introduction to Boundary Layer Meteorology.* Kluwer Academic Publishers, Dordrecht, The Netherlands. 666 pp.

Thompson, W. T., and S. D. Burk, 1993: Postfrontal boundary-layer modification over the western Gulf of Mexico during GUFMEX. *J. Appl. Meteor.*, **32**, 1521-1537.

Troen, I. B., and L. Mahrt, 1986: A simple model of the atmospheric boundary layer; sensitivity to surface evaporation. *Bound.-Layer Meteor.*, **37**, 129-148.

Biographical Sketch

Craig T. Sloan was born in New York, New York, on 27 May 1968. He attended Johns Hopkins University and received a Bachelor of Arts in Earth and Planetary Sciences in 1989. Upon receipt of his degree, he was commissioned as a second lieutenant in the United States Air Force. He was initially assigned to the Basic Meteorology Program at Florida State University where he received a Certificate of Meteorology in 1991. After being stationed at Mather AFB, CA, he then returned to Florida State University in 1992 to pursue a Master of Science in Meteorology under the auspices of the Air Force Institute of Technology.